

UNIVERSITÀ DEGLI STUDI DI MILANO

FACOLTÀ DI SCIENZE MATEMATICHE, FISICHE E NATURALI
CORSO DI LAUREA MAGISTRALE IN FISICA



ABELIAN SANDPILE MODELS
AND
SAMPLING OF TREES AND FORESTS

Relatore:

Prof. Sergio CARACCIOLO

Correlatore:

Dott. Andrea SPORTIELLO

P.A.C.S.: 05.65.b

Tesi di laurea di:

Guglielmo PAOLETTI

Matr. Nr 686472

Anno Accademico 2006–2007

a Lucia

Contents

1	Trees and Forests	1
1.1	Graph theory	1
1.1.1	Basic definitions	1
1.1.2	Algebraic graph theory	3
1.2	Kirchhoff theorem for spanning trees	4
1.3	Potts model	8
1.3.1	Model	8
1.3.2	Fortuin-Kasteleyn representation	8
1.3.3	Limit $q \rightarrow 0$	9
1.4	Applications of spanning trees and forests	10
1.4.1	Bijection dimer-covering \leftrightarrow spanning-trees	10
1.4.2	Temperley-Lieb algebra, trees and forests	11
2	The Abelian Sandpile model	17
2.1	General properties	17
2.2	The abelian group	21
2.3	The evolution operator and the steady state	22
2.4	Recurrent and transient configurations	23
2.4.1	The multiplication by identity test	23
2.4.2	Burning test	24
2.5	Algebraic aspects	27
2.5.1	Toppling invariants	27
2.5.2	Rank of \mathcal{G} for a rectangular lattice	30
3	Cluster-toppling rules and exotic operators	33
3.1	Generalized toppling rules	33
3.2	The operator $N_i = a_i^\dagger a_i$	40
3.2.1	The ASM-propagators	42
3.3	Stationary state	49
4	An algorithm for uniform sampling of trees	53

5	Monte-Carlo algorithms for the Potts model	57
5.1	Swendsen-Wang algorithm	57
5.2	Chayes-Machta algorithm	58
5.3	Sweeny algorithm	59
5.4	Region $q < 1$	60
6	Sampling of Forests	61
6.1	Collecting two dynamics together	61
6.2	Boost of slow dynamics	62
6.3	Boost of collected dynamics	63
6.4	Overview on our algorithm	64
6.5	Numerical results	65
	Ringraziamenti	73
	Bibliography	77

1. Trees and Forests

1.1 Graph theory

1.1.1 Basic definitions

A graph is a mathematical structure made up of points and lines. Some pairs of points may be joined by lines. The same pair of points may eventually be joined by several lines, so a graph may have multiple edges, and eventually some lines may connect a point to itself forming a “loop”. This kind of pathological situations are not relevant for most cases, so we define a graph to be *simple* when it has no multiple lines or loops; in the following we will discuss simple graphs, unless otherwise stated.

A graph G is defined as a pair (V, E) of sets such that $E \subseteq [V]^2$. The elements of V are *vertices* (or *points* or *sites* or *nodes*) and the elements of E are *edges* (or *bond* or *link* or *lines*). A graph with vertex set V is said to be a graph on V . The vertex set of a graph is referred to as $V(G)$ and the edge set $E(G)$, this convention is independent of any name we had chosen for these sets. We write an edge $e \in E(G)$ as $e = \{x, y\}$, where $x, y \in V(G)$ are two endpoints of the edge, and we can indifferently denote e as $\{x, y\}$ or xy . Two points $x, y \in V(G)$ are said to be *neighbors* or *adjacent* if they are connected by an edge (xy is an edge of G) and the edge xy is said to be incident on x and y (and vice-versa). We call S a subgraph of G if $S = (V', E')$ with $V' \subseteq V$, $E' \subseteq E$ and V' containing all the vertices adjacent to E' . If $V(G) = V(S)$ we say that S is *spanning* in G . The set of spanning subgraphs for a graph G is in natural bijection with the set of subsets of $E(G)$, which has a vector-space structure on \mathbb{Z}_2 with the sum defined as the symmetric difference of the subsets, $E_1 \triangle E_2 = (E_1 \cup E_2) \setminus (E_1 \cap E_2)$.

The *degree* (or *valency*) $d_G(v) = d(v)$ of a vertex v is the number of edges in $E(G)$ incident on that vertex. The subscript denotes the graph when not clear, for example, in the case above of $S \subseteq G$, we would also have that $d_S(v) \leq d_G(v)$ is the number of edges in $E(S)$ incident on v . If all vertices of G have the same degree k , the graph G is *k-regular* or simply *regular*. We call an Eulerian subgraph (more shortly a *loop*) L a subgraph with $d_L(v)$ even for all $v \in V(L)$, the vector-subspace \mathcal{L} on \mathbb{Z}_2 of these subgraphs has dimension $L(G)$ which is the number of *independent loops* in G .

A *path* in a graph is a subgraph $P = (V, E)$ on the form:

$$V = \{x_0, x_1, \dots, x_\ell\} \quad E = \{x_0x_1, x_1x_2, \dots, x_{\ell-1}x_\ell\} \quad (1.1)$$

where x_k are all distinct; the path P is usually denoted as the sequence of its vertices, x_0, x_1, \dots, x_ℓ . We say that this is a path from x_0 to x_ℓ and the number of edges of the path is its length.

A graph G is said to be connected if for every pair of vertices in G there exists a path joining them. If P is a path with vertices $x_0, x_1, \dots, x_{\ell-1}$, $\ell \geq 3$ and $x_0 x_{\ell-1}$ is in $E(G)$, then $C := P + x_{\ell-1} x_0$ is a *cycle* in G ; so a cycle $C = (V, E)$ is in the form

$$V = \{x_0, x_1, \dots, x_{\ell-1}\} \quad E = \{x_0 x_1, x_1 x_2, \dots, x_{\ell-1} x_0\} \quad (1.2)$$

with all $x_0, x_1, \dots, x_{\ell-1}$ distinct. A graph (or a subgraph) without any cycle is a *forest* or an *acyclic* graph; a *tree* is a connected forest, note that in a forest every component is a tree.

If the edges are ordered pairs of vertices we get the notion of *directed* graph. An ordered pair (a, b) is said to be an edge directed from a to b , or an edge beginning at a and ending at b , and can be denoted as usual as ab , while note however that in this case $ab \neq ba$.

For every graph is valid the *Euler formula*, which relates the number of vertices, $|V|$, the number of edges, $|E|$, the number of connected components, C , and the number of independent loops, L :

$$|V| + L = |E| + C \quad (1.3)$$

For trees, in which $C = 1$ and $L = 0$, the Euler formula reduces to:

$$|V| = |E| + 1 \quad (1.4)$$

We call a *planar embedding* for a graph a function that maps each vertex of a graph G to a distinct point of \mathbb{R}^2 , and each edge of G to a continuous non self-intersecting curve in the plane joining its endpoints, such that curves corresponding to nonincident edges do not meet, and curves corresponding to incident edges meet only in the point representing their common vertex. A graph is *planar* iff has a planar embedding. More generally, we call an *embedding onto a surface of genus g* the analogue of above, with \mathbb{R}^2 replaced with the genus- g torus equipped with a whatever structure of differentiable manifold, and we say that G is of genus g , if g is the minimum value for which such an embedding exists. However, all of this “continuum” structure is to many extents redundant: as we are only interested to the topological properties of these embeddings, not on the metric properties, we could alternatively define planarity and genus of a graph through the structure of 2-dimensional cell complexes, which leads to the definition of elementary *faces*, or *plaquettes*, in the cell complex, which are cycles of G containing no other vertices of G “inside”, on one of the two sides, w.r.t. the embedding.

Given a planar graph G we can form a special graph, the *dual graph* G^* . The vertices of G^* correspond to the faces of G , with each vertex placed in the corresponding face. Every edge e of G gives rise to an edge of G^* joining the two faces of G containing e (fig. 1.1). We can now define a correspondence from the set of

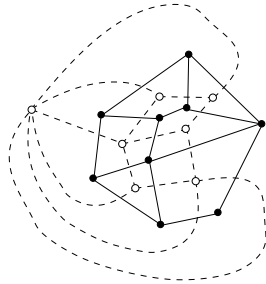


Figure 1.1 Example of graph (black dots and solid lines) and the corresponding dual graph (white dots and dashed lines)

spanning subgraph of G to the set of spanning subgraphs of G^* . To the subgraph $S = (V, E)$ we associate $S^* = (V^*, E^*)$, where $V^* = V(G^*)$ and $e \in E^*$ are chosen such that for every pair edge–dual-edge (e, e^*) , either $e \in E$ and $e^* \notin E^*$ or $e \notin E$ and $e^* \in E^*$. It follows that a loop in a subgraph of G encircles a connected component in the associated subgraph of G^* , and vice-versa; so we have, denoting with D the transformation of duality, the following relations:

$$\begin{array}{ccc} \text{connected subgraphs} & \xrightarrow{D} & \text{subgraphs without loops} \\ \text{subgraphs without loops} & \xrightarrow{D} & \text{connected subgraphs} \end{array} \quad (1.5)$$

This implies that a spanning tree of G , for definition without loops and connected, has as counterpart in G^* a spanning tree, thus there are as many spanning trees in the graph G as in its dual G^* .

1.1.2 Algebraic graph theory

The Algebraic graph theory aims to translate properties of graphs into algebraic properties of associated structures and then, using these ones, to deduce theorems about graphs. We introduce here some basic concepts, for a more detailed review see [14, 16].

For a given graph G with n vertices and m edges, we define its *adjacency matrix* $A(G)$ as an $n \times n$ matrix whose entries a_{ij} are given by:

$$a_{ij} = \begin{cases} 1 & \text{if } i \text{ and } j \text{ are adjacent} \\ 0 & \text{otherwise} \end{cases} \quad (1.6)$$

It follows from the definition that, for an undirected graph, A is a real symmetric matrix, with trace 0. We are interested primarily in the properties of the adjacency matrix which are invariant under permutations of rows and columns, i.e. a relabelling of vertices. The foremost among them are the spectral property of this matrix. Suppose the characteristic polynomial of $A(G)$ can be written as:

$$\chi(G; \lambda) = \lambda^n + c_1 \lambda^{n-1} + c_2 \lambda^{n-2} + \cdots + c_n \quad (1.7)$$

then the coefficients c_i are the sum of the principal minors of A . The first few of them can be easily proved to be:

1. $c_1 = 0$
2. $-c_2$ is the number m of edges in G
3. $-c_3$ is twice the number of triangles in G
- ...

We define the *incidence matrix* $D(G)$ of a directed graph as the $n \times m$ matrix with rows and columns indexed by vertices and edges whose entries d_{ie} are given by:

$$d_{ie} = \begin{cases} +1 & \text{if the arrow } e \text{ starts from } i \\ -1 & \text{if the arrow } e \text{ ends in } i \\ 0 & \text{otherwise} \end{cases} \quad (1.8)$$

We define the coordination matrix of the graph $C(G)$ as the diagonal matrix $n \times n$ whose entries C_{ii} are given by the valency of the i -th vertex.

It can be proved that:

$$DD^T = C - A \quad (1.9)$$

and DD^T is independent of the orientation. We call this $n \times n$ matrix $\Delta = DD^T$ the “unweighted” *Laplacian matrix*, as it corresponds to the Laplacian operator for regular lattices. If we *weight* each pair of sites ij with w_{ij} , which is a formal algebraic variable, we can define the “weighted” Laplacian matrix, as the matrix with entries Δ_{ij} defined by:

$$\Delta_{ij} = \begin{cases} -w_{ij} & \text{for } i \neq j \\ \sum_{k \neq i} w_{ik} & \text{for } i = j \end{cases} \quad (1.10)$$

We note that the sum over the elements in a row or in a column is always equal to zero, so the matrix annihilates the vector $(1, 1, \dots, 1)$. Since Δ has an eigenvector with eigenvalue zero, it follows that $\det \Delta = 0$.

1.2 Kirchhoff theorem for spanning trees

A classical result of algebraic graph theory is the matrix-tree theorem, first discovered by Kirchhoff [13] in the theory of electric circuits. For any vertex $i \in V$ we let $\Delta(i)$ be the matrix obtained by Δ deleting the i -th row and column. In its simplest formulation the Kirchhoff theorem states that the number of spanning trees for a graph is given by $\det \Delta(i)$; more generally, in the case of weighted Laplacian, the theorem puts in relation the generating polynomial for trees, $Z_{\mathcal{T}}(\vec{w})$, with the determinant of minors of the Laplacian matrix:

$$Z_{\mathcal{T}}(\vec{w}) = \sum_{T \in \mathcal{T}} \prod_{e \in T} w_e = \det \Delta(i) \quad (1.11)$$

where \mathcal{T} denotes the set of spanning trees of the graph G . The i independence of $\det \Delta(i)$ expresses, in electrical-circuit language, that is physically irrelevant which site i is chosen to be the “ground”, and, in graph theory, that is irrelevant which site is chosen as “root” to obtain all the possible spanning trees.

More generally, for any set of vertices $I, J \subseteq V$, let $\Delta(I|J)$ be the matrix obtained from Δ by deleting the rows indexed by I and the columns indexed by J , for $I = J$ we write simply $\Delta(I)$. If $I = (i_1, i_2, \dots, i_r)$ with $0 \leq i_j \leq |V|$ we write the *principal-minors matrix tree theorem* as follows:

$$\det \Delta(I) = \det \Delta(i_1, i_2, \dots, i_r) = \sum_{F \in \mathcal{F}(i_1, i_2, \dots, i_r)} \prod_{e \in F} w_e \quad (1.12)$$

where $\mathcal{F}(i_1, i_2, \dots, i_r)$ denotes the set of spanning forests of G composed of r disjoint trees, each one with exactly one root vertex chosen between the vertices i_1, i_2, \dots, i_r . This theorem is easily derived by the simple matrix-tree theorem considering the graph in which all the sites i_1, i_2, \dots, i_r are contracted in a single site. The last theorem we recall is the *all-minors matrix-tree theorem*, it states that, for $|I| = |J|$:

$$\det \Delta(I|J) = \sum_{F \in \mathcal{F}(I|J)} \prod_{e \in F} w_e \quad (1.13)$$

where $\mathcal{F}(I|J)$ denotes the set of spanning forests in G with r components, each of which has exactly one site from I and one from J , possibly the same vertex.

We can now introduce, for each site $i \in V$, a pair of Grassmann variables ψ_i and $\bar{\psi}_i$. These variables are nilpotent ($\psi_i^2 = \bar{\psi}_i^2 = 0$), anticommute and obey the usual rules for Grassmann integration [21]. We then have for every matrix A , using the notation $\mathcal{D}(\psi, \bar{\psi}) = \prod_{i \in V} d\psi_i d\bar{\psi}_i$, the following relation to compute the determinant:

$$\int \mathcal{D}(\psi, \bar{\psi}) e^{\bar{\psi} A \psi} = \det A \quad (1.14)$$

and more generally:

$$\int \mathcal{D}(\psi, \bar{\psi}) \psi_{i_1} \bar{\psi}_{j_1} \dots \psi_{i_r} \bar{\psi}_{j_r} e^{\bar{\psi} A \psi} = \epsilon(i_1, \dots, i_r | j_1, \dots, j_r) \det A(i_1, \dots, i_r | j_1, \dots, j_r) \quad (1.15)$$

where the sign $\epsilon(I|J)$ is defined as $\epsilon(I|J) = (-1)^{\sum I + \sum J}$ if the sites are ordered ($i_1 < i_2 < \dots < i_r$ and the same for J), obviously it is always +1 when $(i_1, \dots, i_r) = (j_1, \dots, j_r)$. At this point it is possible to rewrite the matrix-tree theorem (1.11) using the Grassmann variables we have just introduced, obtaining:

$$\det \Delta(0) = \int \mathcal{D}(\psi, \bar{\psi}) \bar{\psi}_0 \psi_0 e^{\bar{\psi} \Delta \psi} = \sum_{T \in \mathcal{T}} \prod_{e \in T} w_e \quad (1.16)$$

It is possible to derive this result without using the well-known links between matrix-determinant and Grassmann integrations, showing directly how the details

of the integration lead to have on the r.h.s. the sum over the spanning trees. The result obtained for the trees, using the root in 0, can be easily extended to more complex roots. For example we can also have a edge-root (say ij), and so obtain:

$$\int \mathcal{D}(\psi, \bar{\psi}) (\bar{\psi}_i \psi_i \bar{\psi}_j \psi_j) e^{\bar{\psi} \Delta \psi} \quad (1.17)$$

or we can fix a set of r vertices root

$$\int \mathcal{D}(\psi, \bar{\psi}) \prod_{\alpha=1}^r (\bar{\psi}_{i_\alpha} \psi_{i_\alpha}) e^{\bar{\psi} \Delta \psi} \quad (1.18)$$

At this point it is possible to rewrite also the principal-minors matrix tree theorem (1.12) in the form:

$$\int \mathcal{D}(\psi, \bar{\psi}) \prod_{\alpha=1}^r (\bar{\psi}_{i_\alpha} \psi_{i_\alpha}) e^{\bar{\psi} \Delta \psi} = \sum_{F \in \mathcal{F}(i_1, i_2, \dots, i_r)} \prod_{e \in F} w_e \quad (1.19)$$

Now we follow the derivation proposed in [1], to construct an interesting fermionic model. Let us introduce, for each subgraph $\Gamma = (V_\Gamma, E_\Gamma)$ of G , the operator:

$$Q_\Gamma = \left(\prod_{e \in E_\Gamma} w_e \right) \left(\prod_{i \in V_\Gamma} \bar{\psi}_i \psi_i \right) \quad (1.20)$$

These operators are even and so commute with each other, and with the entire Grassmann algebra. We now consider the family $\mathbf{\Gamma} = \{\Gamma_1, \dots, \Gamma_\ell\}$ with $\ell \geq 0$ and try to evaluate the integral of the form:

$$\int \mathcal{D}(\psi, \bar{\psi}) Q_{\Gamma_1} \dots Q_{\Gamma_\ell} e^{\bar{\psi} \Delta \psi} \quad (1.21)$$

First we note that if some of the Γ_i 's have some vertex in common, then the integral vanishes for the property of nilpotency of the Grassmann variables. In the case the Γ_i 's are vertex disjoint, then we know how to evaluate the integral using the formula (1.19). In fact we can write:

$$\int \mathcal{D}(\psi, \bar{\psi}) \left(\prod_{k=1}^{\ell} \prod_{i \in V_{\Gamma_k}} \bar{\psi}_i \psi_i \right) e^{\bar{\psi} \Delta \psi} = \sum_{F \in \mathcal{F}(\cup_k V_{\Gamma_k})} \prod_{e \in F} w_e. \quad (1.22)$$

When using this expression to solve the integral (1.21), the edges in $E_\Gamma = \cup_k E_{\Gamma_k}$ cannot be in any forest, otherwise the integral would vanishes for the nilpotency of the Grassmann variables. However adding $\prod_{e \in E_\Gamma} w_e$ on the r.h.s. of the previous equality we note that each forest can be put into one-to-one correspondence with $\mathbf{\Gamma}$ -forests, that are subgraphs of G spanning with ℓ components, each one with

exactly one Γ_i and with no cycles except the ones in Γ_i . So we can rewrite the (1.21) as follows:

$$\int \mathcal{D}(\psi, \bar{\psi}) Q_{\Gamma_1} \dots Q_{\Gamma_l} e^{\bar{\psi} \Delta \psi} = \sum_{H \in \mathcal{F}_\Gamma} \prod_{e \in H} w_e \quad (1.23)$$

Introducing now a coupling constant t_Γ for each connected subgraph Γ of G , and using the relation $1 + t_\Gamma Q_\Gamma = e^{t_\Gamma Q_\Gamma}$, given by the properties of Grassman integration, we have:

$$\int \mathcal{D}(\psi, \bar{\psi}) e^{\bar{\psi} \Delta \psi + t_\Gamma Q_\Gamma} = \sum_{\substack{\Gamma \text{ vertex-} \\ \text{disjoint}}} \left(\prod_{\Gamma \in \mathbf{\Gamma}} t_\Gamma \right) \sum_{H \in \mathcal{F}_\Gamma} \prod_{e \in H} w_e \quad (1.24)$$

Interchanging the summation over H and $\mathbf{\Gamma}$ it is possible to rewrite this expression in a different form. We consider a spanning subgraph H of G with l connected components H_1, \dots, H_l and we say that Γ marks H_i , $\Gamma \prec H_i$, if H_i contains Γ and has no cycles except those lying entirely in Γ , we also define the weight for H_i as:

$$W(H_i) = \sum_{\Gamma \prec H_i} t_\Gamma \quad (1.25)$$

In this framework the property of H to be a $\mathbf{\Gamma}$ -forest is equivalent to say that each of its components is marked exactly by one of the Γ_i , so we can rewrite the (1.24) as follows:

$$\int \mathcal{D}(\psi, \bar{\psi}) e^{\bar{\psi} \Delta \psi + t_\Gamma Q_\Gamma} = \sum_{\substack{H \text{ spanning} \subseteq G \\ H = (H_1, \dots, H_\ell)}} \left(\prod_{i=1}^{\ell} W(H_i) \right) \prod_{e \in H} w_e \quad (1.26)$$

This is the general combinatorial formula.

We now make a particular choice for the Γ 's and the related t_Γ , say that:

- (i) $t_\Gamma = t$ whenever Γ consists of a single vertex with no edge;
- (ii) $t_\Gamma = u$ whenever Γ consists of two vertices connected by a single edge;
- (iii) $t_\Gamma = 0$ otherwise;

So we have:

$$\int \mathcal{D}(\psi, \bar{\psi}) \exp \left[\bar{\psi} \Delta \psi + t_\Gamma Q_\Gamma \right] = \sum_{\substack{F \in \mathcal{F} \\ F = (F_1, \dots, F_\ell)}} \left(\prod_{i=1}^{\ell} (t|V_{F_i}| + u|E_{F_i}|) \right) \prod_{e \in F} w_e \quad (1.27)$$

where \mathcal{F} denotes the set of spanning forests of G . Since $|V_{F_i}| - |E_{F_i}| = 1$ for each tree, we can take $u = -t$ and obtain the generating function for *unrooted* spanning forest with weight t for each component.

1.3 Potts model

1.3.1 Model

The most famous model in statistical mechanics is the *Ising* model, a lattice model where on each site there is a spin variable that takes its value in $\{0, 1\}$ (or (\uparrow, \downarrow) , or (white, black)) and interacts with its nearest-neighbors; the Potts model is its direct generalization to the case of spins which take q values.

Let $G = (V, E)$ be a graph, on each site $i \in V$ we define a spin variable $\sigma_i \in \{1, \dots, q\}$ where $q \in \mathbb{N}_+$ (the Ising model is the case for $q = 2$) and for each edge $e \in E$ we define a coupling constant $J_e \in \mathbb{R}$. The interaction of the model is given by a delta-function for each edge $e = ij$, of the form $-J_e \delta(\sigma_i, \sigma_j)$. Denoting the spin configuration of the system as $\sigma = \{\sigma_i\}_{i \in V}$ we can write the Hamiltonian of the Potts model on G as:

$$\mathcal{H}(\sigma) = - \sum_{ij=e \in E} J_e \delta(\sigma_i, \sigma_j) \quad (1.28)$$

The partition function of the model is $Z_{Potts} = \sum_{\sigma} e^{-\beta \mathcal{H}(\sigma)}$, the sum of the Boltzmann weights, $e^{-\beta \mathcal{H}}$, for each possible configuration. If we call $v_e = e^{\beta J_e} - 1$ and $\mathbf{v} = \{v_e\}_{e \in E}$ we can rewrite the partition function as dependent on q and \mathbf{v} as follows:

$$Z_G(q, \mathbf{v}) = \sum_{\sigma} \prod_{e \in E} [1 + v_e \delta(\sigma_i, \sigma_j)] \quad (1.29)$$

Let now suppose J_e to be constant, $J_e = J$, for all the edges. The model is said to be *ferromagnetic* if $J \geq 0$ ($v \geq 0$), *anti-ferromagnetic* if $-\infty \leq J \leq 0$ ($-1 \leq v \leq 0$) and *unphysical* when $v \notin [-1, \infty)$, due to the fact that in this last region the Boltzmann weight is no more positive, as expected for a statistical mechanics model.

1.3.2 Fortuin-Kasteleyn representation

It is possible to give a subgraph expansion for the partition function of the Potts model, this expansion was first discovered by Fortuin and Kasteleyn [17] in 1972. Using this form, the partition function of the model is found to be a polynomial in q and \mathbf{v} , and has the particular feature to allow an analytic continuation in the parameter q .

Using the relation:

$$\sum_{A \subseteq E} \prod_{e \in A} v_e = \prod_{e \in E} (1 + v_e) \quad (1.30)$$

in the partition function (1.29) we obtain:

$$\begin{aligned}
Z_G(q, \mathbf{v}) &= \sum_{\sigma} \prod_{e \in E} [1 + v_e \delta(\sigma_i, \sigma_j)] \\
&= \sum_{\sigma} \sum_{A \subseteq E} \prod_{e \in A} v_e \delta(\sigma_i, \sigma_j) \\
&= \sum_{A \subseteq E} q^{C(A)} \prod_{e \in A} v_e
\end{aligned} \tag{1.31}$$

where $C(A)$ is the number of connected components of A subgraph of G (considered together with the set of vertices V of the whole graph G). The equality between the second and the third line is obtained summing over the configurations with the delta constraint. This expression shows how the partition function of the q -state Potts model, defined separately for each integer value of q , is in fact the restriction to \mathbb{N}_+ of a polynomial in q , so we define, in analytic continuation, the *Fortuin-Kasteleyn Random-Cluster partition function* which is the algebraic function

$$Z_G(q, \mathbf{v}) = \sum_{A \subseteq E} q^{C(A)} \prod_{e \in A} v_e \tag{1.32}$$

Further on, using the Euler relation (1.3), and noting that the subgraphs A we are using are spanning, in fact in (1.30) we use subset of only the edge set, we can rewrite the $Z_G(q, \mathbf{v})$ in the form:

$$Z_G(q, \mathbf{v}) = q^{|V|} \sum_{A \subseteq E} q^{L(A)} \prod_{e \in A} \frac{v_e}{q} \tag{1.33}$$

where $L(A)$ denotes the number of independent cycles of A . The resulting probability measure on 2^E is called the *Fortuin-Kasteleyn random-cluster model*. This framework is very useful trying to obtain Monte Carlo algorithms for sampling the model.

1.3.3 Limit $q \rightarrow 0$

Having now the possibility to study the partition function of the Potts model for arbitrary values of q and v we face the task of obtaining the limit for $q \rightarrow 0$. We follow two different ways to obtain a meaningful limit.

First we take $q \rightarrow 0$ with fixed \mathbf{v} . By the result (1.32) we see that performing the limit in this way we are selecting the subgraphs $A \subseteq E$ with the smallest possible number of connected components, the minimum number achievable for $C(A)$ is obviously $C(G)$, i.e. simply 1 in the case G is connected. We thus have:

$$\lim_{q \rightarrow 0} q^{C(G)} Z_G(q, \mathbf{v}) = C_G(\mathbf{v}) \tag{1.34}$$

where

$$C_G(\mathbf{v}) = \prod_{\substack{A \subseteq E \\ C(A)=C(G)}} \prod_{e \in A} v_e \tag{1.35}$$

is the generating polynomial of “maximally connected spanning subgraphs”.

A different limit can be obtained taking $q \rightarrow 0$ with $\mathbf{w} = \mathbf{v}/q$ fixed. By the result (1.33) we see that we are selecting the subgraphs $A \subseteq E$ with the smallest possible number of independent cycles, which has minimum value 0, for the forests. We therefore can write:

$$\lim_{q \rightarrow 0} q^{-|V|} Z_G(q, q\mathbf{w}) = F_G(\mathbf{w}) \quad (1.36)$$

where

$$F_G(\mathbf{w}) = \sum_{\substack{A \subseteq E \\ L(A)=0}} \prod_{e \in A} w_e \quad (1.37)$$

is the generating polynomial of spanning forests. Finally we suppose to replace, in $C_G(\mathbf{v})$, v_e by λv_e and then take $\lambda \rightarrow 0$. This select out, among the possible subgraphs, the ones with fewest edges: these are the maximal spanning forests (or spanning trees in the case G is connected), they have exactly $|V| - C(G)$ edges. So we have:

$$\lim_{\lambda \rightarrow 0} \lambda^{C(G)-|V|} C_G(\lambda\mathbf{v}) = T_G(\mathbf{v}) \quad (1.38)$$

where

$$T_G(\mathbf{v}) = \sum_{\substack{A \subseteq E \\ C(A)=C(G) \\ L(A)=0}} \prod_{e \in A} v_e \quad (1.39)$$

is the generating polynomial for maximal spanning forests (we use here the letter T because in most cases we deal with connected graphs, and consequently with spanning trees). Suppose then to replace \mathbf{w} in (1.37) with $\lambda\mathbf{w}$ and then to take $\lambda \rightarrow \infty$, this select out the subgraphs with greatest number of edges, among the spanning forests, i.e. the maximal spanning forests. So we have:

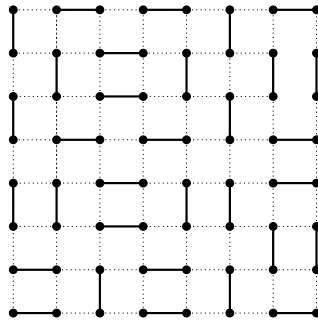
$$\lim_{\lambda \rightarrow \infty} \lambda^{C(G)-|V|} F_G(\lambda\mathbf{w}) = T_G(\mathbf{v}) \quad (1.40)$$

In summary a certain double-limit of the partition function for the q -state Potts model in the limit $q \rightarrow 0$ is the generating polynomial for spanning trees of the graph on which is defined the model, while the single sides of these limit procedures give respectively spanning forests and connected spanning subgraphs (which are indeed dual ensembles in the special case of planar graphs).

1.4 Applications of spanning trees and forests

1.4.1 Bijection dimer-covering \leftrightarrow spanning-trees

A *dimer covering* for a given graph G is a collection of edges that covers all the vertices exactly once, that is, each vertex is adjacent to a unique edge; in other words is a pairing of adjacent vertices (fig. 1.2).

Figure 1.2 dimer covering for a 8×8 square lattice

There exists a bijection, due to Temperley [23], between the spanning trees on a planar graph and dimer coverings of a suitable associated graph. Let us consider a planar graph G , we then define the planar graph $G' = (E', V')$, where V' is obtained as the union of the set of vertices $V(G)$ of graph G , the set of vertices $V(G^*)$ of the dual graph G^* and the set \tilde{V} of vertices defined as the planar intersections between pairs of edges (e, e') , with $e \in E(G)$, and $e' \in E(G^*)$. E' is the set of edges such that for each $e = ij \in E(G)$ there are two edges in E' , $e_1 = ij'$ and $e_2 = j'j$ where j' is the intersection between edge e and the corresponding dual, and analogously

for the dual edges, 

The bijection associates to a spanning tree of the graph G a dimer covering of the graph G' , with a vertex in $V(G)$ and a vertex in $V(G^*)$ removed. Given a spanning tree in G and a vertex $v \in V(G)$ we direct each edge in the spanning tree toward this vertex and label the half-edge in E' of e farther from v with 1 and the other half with 2. Then we choose as dimer, for each edge $e \in E(G)$, the half labelled by 1. Repeating then the same procedure for the corresponding spanning tree of the dual graph G^* with respect to its removed vertex $v' \in V(G^*)$ we obtain the dimer covering of $G' \setminus \{v, v'\}$.

In particular for a portion of the square lattice, this procedure associates to each $n \times n$ lattice a $(2n - 1) \times (2n - 1)$ lattice with one site removed (e.g. the top right corner), the site removed from the dual lattice is intended to be the vertex corresponding to the external face. In fig. 1.3 the spanning tree S of G is in red and the dual counterpart S^* is in blue, all the outgoing edges of S^* are intended to meet in the removed vertex of the dual graph. Following the just displayed procedure it is possible to obtain the dimer covering.

1.4.2 Temperley-Lieb algebra, trees and forests

An interesting model in statistical mechanics is the $O(n)$ loop model [20]; this is a lattice model where on each site i is defined a spin variable \vec{s}_i , which belongs to an n -dimensional sphere of radius 1 ($|s_i| = 1$) with some spherically symmetrical measure: $\vec{v}_i \in \mathbb{R}^n$; $d\mu(\vec{s}_i) = d\mu(R \cdot \vec{s}_i)$ with $R \in O(n)$. With $\int d\vec{s}_i$ we denote the

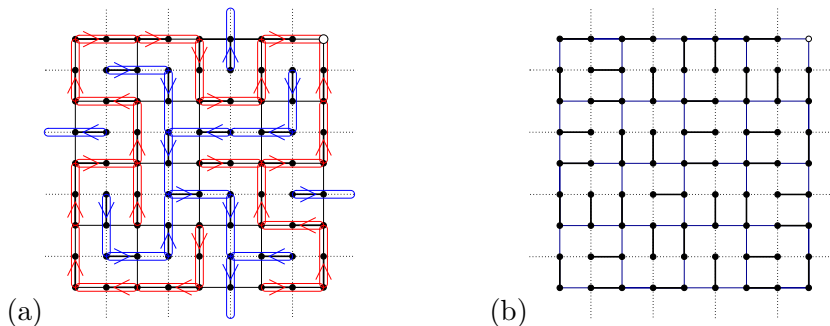


Figure 1.3 Spanning tree for a 5×5 square lattice (a) and the associated dimer covering for the 9×9 square lattice with a site removed (b). The direct graph is displayed in blue and the dual with dashed lines.

measure on the sphere and we intend the inner product of the spin variables as:

$$\vec{s}_i \cdot \vec{s}_j = \sum_{\alpha=1}^n s_i^{(\alpha)} s_j^{(\alpha)} \quad (1.41)$$

The model is then defined by the partition integral:

$$Z_{O(n)} = \int \prod_{\ell} d\vec{s}_{\ell} \prod_{\langle ij \rangle} (1 + n\beta \vec{s}_i \cdot \vec{s}_j) \quad (1.42)$$

where n is the dimension of the sphere, β a parameter depending on the temperature and the second product is intended on pair of sites nearest-neighbors. For a lattice with vertex coordination k , it will turn out that only momenta up to k of the measure $d\mu$ are relevant.

It is easy to compute the momentum of the spin variables using the spherical measure (denoted with $\langle \cdot \rangle$), for the symmetry of the measure only even-momenta are non-null and the maximum momentum different from zero is the one of order k . Thus, restricting to a lattice of coordination 3, the following equalities are found to be true:

$$\langle 1 \rangle = 1 \quad (1.43a)$$

$$\langle s_i^{(\alpha)} \rangle = 0 \quad (1.43b)$$

$$\langle s_i^{(\alpha)} s_i^{(\beta)} \rangle = \frac{1}{n} \delta_{\alpha\beta} \quad (1.43c)$$

$$\langle s_i^{(\alpha)} s_i^{(\beta)} s_i^{(\gamma)} \rangle = 0 \quad (1.43d)$$

Let us say that an edge ij is *marked* with “colour” α when its endpoints are either with the component $n_i^{(\alpha)} = n_j^{(\alpha)} \neq 0$ and is *unmarked* when its endpoints has different components. We can expand the product in (1.42) and note that the integration forces the 3 edges incident on the same vertex to be:

- two marked with the same colour
- one unmarked or every edge unmarked.

Thus the only allowed configurations with contribution different from zero are the ones with loops of edges marked with the same colour, with n colours available; they give a contribution $n^c \beta^L$ where c is the number of loops and L the count of edges constructing the various loops. At this point we can rewrite $Z_{O(n)}$ in a purely combinatorics form, summing over the different loop-diagrams, G , as follows:

$$Z_{O(n)} = \sum_G \beta^L n^c. \tag{1.44}$$

In this case, the limit $\beta \rightarrow \infty$ and $n \rightarrow 0$, corresponds to select among the allowed configurations the ones with the maximum number of occupied edges, and the minimum number of loops, 1 when possible.

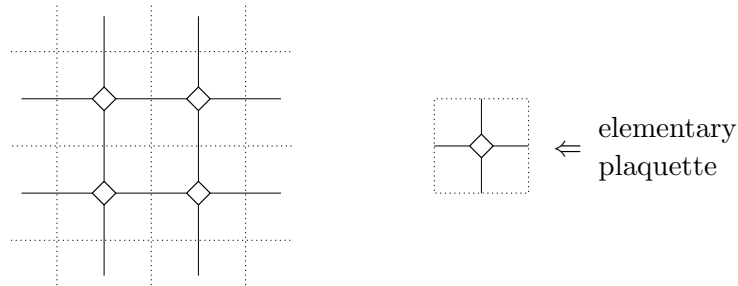


Figure 1.4 square-octagonal lattice and its elementary plaquette

Let us set the model in a particular lattice, with coordination 3, composed of squares and octagons (fig. 1.4); let E be the set of edges belonging only to the octagons and \tilde{E} the set of edges belonging to the squares. It is possible to choose different β 's, say $\tilde{\beta}$ for the edges in \tilde{E} and β for the edges in E . Let now take the limit $\beta \rightarrow \infty$, maintaining $\tilde{\beta}$ constant. In this way we are selecting the configurations with loops composed of the maximum number of edges of the type e , then the limit $n \rightarrow 0$ forces the number of loops to be minimum. The possible structures in each elementary plaquette of the allowed configurations are of just two types:

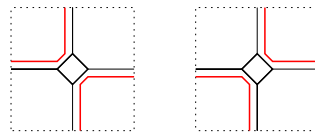
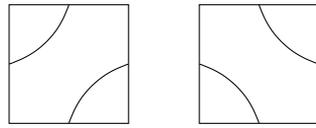


Figure 1.5 allowed configuration for plaquette, where the bonds marked in red are selected

and it is possible to recognize them as part of a Temperley-Lieb algebra.



The elementary faces of the Temperley-Lieb algebra are of two types:

The elements of Temperley Lieb Algebra satisfy some useful relations; indeed, denoting the elementary faces with e_i 's, we can write:

$$\begin{cases} e_i^2 = \lambda e_i \\ e_i e_{i\pm 1} e_i = e_i \end{cases} \quad (1.45)$$

these relations correspond, pictorially, to the following structures:



where λ comes from the dotted closure in the first relation. Finally we note that is easily obtainable a bijection between the configuration of spanning trees or forests in a planar regular graph and a configuration of the loop model in terms of Temperley Lieb plaquettes associated. We consider in the same frame the graph and its dual, then we add a lattice such that each plaquette of the new lattice has vertices in pair belonging to the dual and direct graph and its diagonals are respectively a direct and a dual edge. Then each plaquette corresponds to a different Temperley Lieb elementary face depending on which between the dual and the direct edge is marked as in (fig. 1.6). This gives a one-to-one correspondence between forest configurations and loop configurations of the just defined lattice (fig. 1.7).

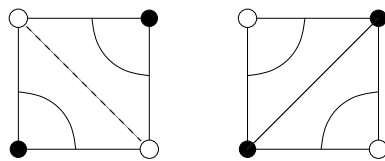


Figure 1.6 two different plaquettes.

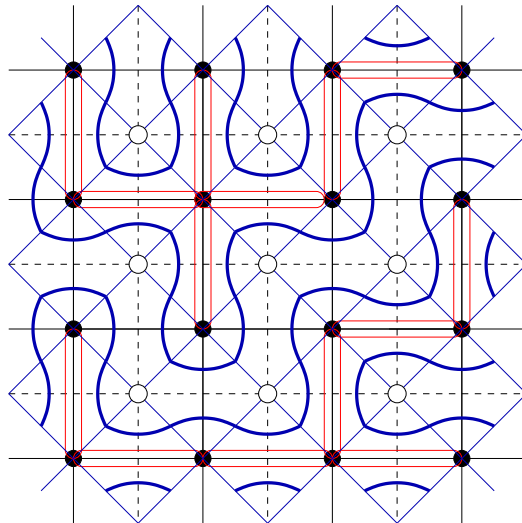


Figure 1.7 Example of loop-model \leftrightarrow spanning tree correspondence.

2. The Abelian Sandpile model

It has been about 20 years since Bak, Tang and Wiesenfeld's landmark papers on self-organized criticality (SOC) appeared [6]. The concept of self-organized criticality has been invoked to describe a large variety of different systems. I shall describe here one specific model: the Abelian Sandpile Model (ASM). The sandpile model was first proposed as a paradigm of SOC and it is certainly the simplest, and best understood, theoretical model of SOC: it is a non-equilibrium system, driven at a slow steady rate, with local threshold relaxation rules, which in the steady state shows relaxation events in bursts of a wide range of sizes, and long-range spatio-temporal correlations. The ASM consists of a special subclass of the sandpile models that exhibits, in the way we will discuss later, the mathematical structure of an abelian group, and permits to obtain a powerful tool in sampling random spanning trees.

2.1 General properties

The ASM is defined as follows [7, 8]: we consider a graph of N sites labelled by integers $i = 1, \dots, N$, at each site we define a nonnegative integer height variable z_i , called the height of the sandpile, and a threshold value $\bar{z}_i \in \mathbb{N}_+$. We define an *allowed* configuration of the sandpile as a set of heights $\{z_i\}$ such that $z_i \geq 0 \quad \forall i$; then we define a *stable* configuration of the sandpile an allowed configuration $\{z_i\}$, such that $z_i < \bar{z}_i \quad \forall i$.

The time evolution of the sandpile is defined using the following rules:

1. *Adding a particle*: Select one of the sites randomly, the probability that the site i is picked being some given value p_i , and add a grain of sand there. Obviously $\sum_i p_i = 1$. On addition of the grain at site i , z_i increases by 1, while the height at the other sites remains unchanged.
2. *Toppling*: If for any site i $z_i \geq \bar{z}_i$, then the site is said to be unstable, it "topples", and lose some sandgrains to other sites. This sandgrain's transfer is defined in terms of an $N \times N$ integer valued matrix Δ , which properties will be specified in (2.2). On toppling at site i , the configuration is updated according to the following rule:

$$z_j \rightarrow z_j - \Delta_{ij} \quad \forall j = 1, \dots, N \quad (2.1)$$

If the toppling results in some other sites becoming unstable, they are also toppled simultaneously (it will be clear in the following that the order of toppling is unimportant). The process continues until all sites become stable (we will see later under which conditions on $\{\bar{z}_i\}$ and Δ the final stability is guaranteed)

At each time step in the evolution, first we add a particle, as specified in rule 1, then we “relax” the configuration, i.e. we perform the necessary topplings to reach a stable configuration as stated in rule 2.

The matrix Δ has the following properties:

$$\Delta_{ii} > 0, \forall i \quad (2.2a)$$

$$\Delta_{ij} \leq 0, \forall i \neq j \quad (2.2b)$$

$$\sum_j \Delta_{ij} \geq 0, \forall i \quad (2.2c)$$

These conditions just ensure that on toppling at site i , z_i must decrease, height at other sites j can only increase and there is no creation of sand in the toppling process. In some sites could be possible to “lose” some sand during a toppling. A site i is said to be “on the boundary” if $\sum_j \Delta_{ij} > 0$, and “in the bulk” if $\sum_j \Delta_{ij} = 0$. Indeed, $\sum_j \Delta_{ij}$ is the total sand lost in the toppling process on i , so that, pictorially, we can think of this “lost sand” as dropping out of some boundary. Clearly, in the formulation on an arbitrary graph, as presented here, this concept of boundary does not need to correspond to some geometrical structure. We note that no stationary state of the sandpile is possible unless the particles can leave the system. The model can be represented by a directed graph on N vertices, where we draw $(-\Delta_{ij})$ directed bonds from site i to j , and $(\sum_j \Delta_{ij})$ arrows from i to outside (fig. 2.1).

In the particular case of square lattice the toppling matrix is given as:

$$\Delta_{ij} = \begin{cases} +4 & \text{if } i = j \\ -1 & \text{if } i, j \text{ are nearest-neighbors} \\ 0 & \text{otherwise} \end{cases} \quad (2.3)$$

In this framework to be on the boundary (or in a corner) has a direct correspondence with the geometrical structure of the lattice.

We assume, without loss of generality, that $\bar{z}_i = \Delta_{ii}$ (this amounts to a particular choice of the origin of the z_i variables). Then we know that if a site i is stable, and the initial conditions for the heights are $z_i(t=0) \geq 0 \forall i \in V$, at all times the allowed values for z_i are the ones for which holds $0 \leq z_i < \bar{z}_i$. This procedure define a Markov chain on the space of stable configurations, with a given equilibrium measure. So running the given dynamics for long times, that means after a large amount of sand added, the system reaches the stationary state. In this state, the relaxation after adding a particle, typically involves a sequence of topplings. This

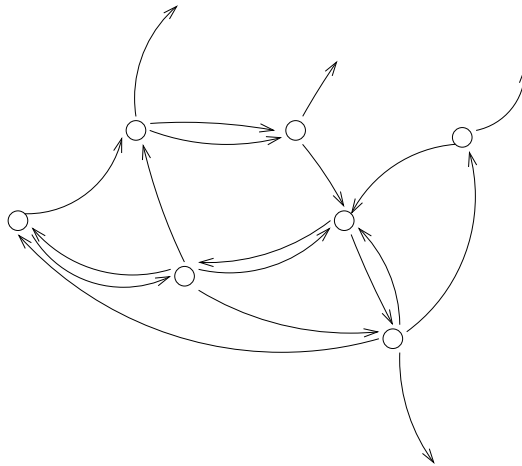


Figure 2.1 a graphical representation of the general ASM. Each node denotes a site. On topplings at any site, one particle is transferred along each arrow directed outward from the site

particular occurrence is called an *avalanche*. The sizes of avalanches can be studied statistically for interesting graphs (e.g. for a partition of \mathbb{Z}^2). In many cases of interest it seems to have a power law tail, which is signal of existence of long-range correlations in the system.

The model has a fundamental abelian property [7]. We define operators a_i 's, which act on the space of the stable configurations of the model, by the following rules: if C is a stable configuration, $a_i C$ is the stable configuration obtained by adding a particle in the site i and then relaxing the system. It is easy to check that starting with an unstable configuration with two or more sites unstable, we get the same final configuration by toppling the sites in a certain order or in another. Let us consider an unstable configuration with the unstable sites α and β , the first toppling of site α leaves β unstable for (2.2b), and, after the toppling of β , we get a configuration in which:

$$z_i \rightarrow z_i - (\Delta_{\alpha i} + \Delta_{\beta i}) \quad \forall i \in V \quad (2.4)$$

this expression is clearly symmetrical under exchange of α and β . Thus we get the same resulting configuration irrespective of whether α or β is toppled first. By repeated use of this argument, we see that in an avalanche, the same final state is reached irrespective of the sequence in which unstable sites are toppled. Also toppling from a site α and then adding a grain in β gives the same result of first adding the grain and then perform the toppling. From this two properties it follows that for all configurations C , and for all i and j , we get $a_i a_j C = a_j a_i C$. In other words the operators a_i commute with each other:

$$[a_i, a_j] = 0 \quad \forall i, j \in V \quad (2.5)$$

Note that, while this property seems very general, it is not shared with most of the other SOC models, even other sandpile models, for example when the toppling

condition depends on the gradient, in this case the inequality (2.2b) would not be satisfied and the operators a_i do not commute.

The operators a_i 's satisfy some other useful relations. For example, on a square lattice, when 4 grains are added at a given site, this is forced to topple once and a grain is added to each of his neighbors. Thus:

$$a_j^4 = a_{j_1} a_{j_2} a_{j_3} a_{j_4} \quad (2.6)$$

where j_1, j_2, j_3, j_4 are the nearest-neighbors of j .

In the general case one has, instead of (2.6),

$$a_j^{\Delta_{ii}} = \prod_{j \neq i} a_j^{-\Delta_{ij}}. \quad (2.7)$$

Using the abelian property, in any product of operators a_i , we can collect together occurrences of the same operator, and using the reduction rule (2.7), it is possible to reduce the power of a_i to be always less than Δ_{ii} . The a_i are therefore the generators of a finite abelian semi-group (in which the associative property follows from their definition) subject to the relation (2.7); these relations define completely the semi-group.

We consider now the repeated action of some given generator a_1 on some configuration C . Since the number of possible states is finite, the orbit of a_i must close on itself, at some stage, so that $a_1^{n+p}C = a_1^n C$ for some positive period p , and non negative integer n . The first configuration that occurs twice in the orbit is not necessarily C , so that the orbit consists of a sequence of transient configurations, followed by a cycle. If this orbit does not exhaust all configurations, we can take a configuration outside this orbit and repeat the process. So the space of all configurations is broken up into disconnected parts, each one containing one limit cycle.

Under the action of a_1 the transient configurations are unattainable once the system has reached one of the periodic configurations. In principle the recurrent configurations might still be reachable as a result of the action of some other operator, say a_2 , but the abelian property implies that if C is a configuration part of one of the limit cycles of a_1 , then so is $a_2 C$, in fact $a_1^p C = C$ implies that $a_1^p a_2 C = a_2 a_1^p C = a_2 C$. Thus the transient configurations with respect to an operator a_1 are also transient with respect to the other operators a_2, a_3, \dots , and hence occur with zero probability in the steady state. The abelian property thus implies that a_2 maps the cycles of a_1 into cycles of a_1 , and moreover that all these cycles have the same period (fig. 2.2). Repeating our previous argument we can show that the action of a_2 on a cycle is finally closed on itself to yield a torus, possibly with some transient cycles, which may be also discarded. Continuing with the same arguments for the other cycles and other generators leads to the conclusion that the set of all the configurations in the various cycles form a set of multi-dimensional tori under the action of the a 's. the configurations that belong to a cycle are said to be *recurrent*, and can be defined, if we allow addition of sand with non zero

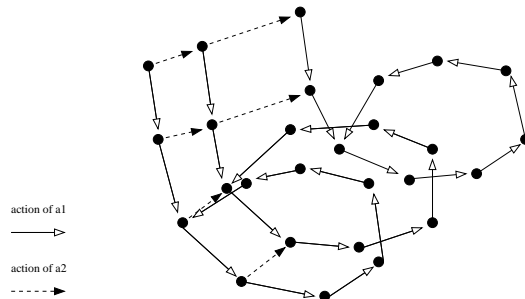


Figure 2.2 graphical representation of the combined action of a_1 and a_2

probability in any site ($p_i > 0 \quad \forall i$), as the configurations reachable by any other configuration with addition of sand followed by relaxation. We denote the set of all recurrent configurations as \mathbf{R} .

2.2 The abelian group

When we restrict our study to the set \mathbf{R} of recurrent configurations, we can define the inverse operator a_i^{-1} for all i , as each configuration in a cycle has exactly one incoming arrow corresponding to the operator a_i . Thus the a_i operators generate a group. The action of the a_i 's on the states correspond to translations of the torus. From the symmetry of the torus under translations, it is clear that all recurrent states occur in the steady state with the same probability.

This analysis, which is valid for every finite abelian group, leaves open the possibility that some recurrent configurations are not reachable from each other, in which case there would be some mutually disconnected tori. However, such a situation cannot happen if we allow addition of sand at all sites with non zero probabilities ($p_i > 0 \quad \forall i$). Let us define C_{max} as the configuration in which all sites have their maximal height, $z_i = \Delta_{ii} - 1 \quad \forall i$. The configuration C_{max} is reachable from every other configuration, is therefore recurrent, and since inverses a_i 's exist for configurations in \mathbf{R} , every configuration is reachable from C_{max} implying that every configuration lie in the same torus.

Let \mathcal{G} be the group generated by operators $\{a_i\}$ i from 1 to N . This is a finite group because the operators a_i 's, due to (2.7), satisfy the closure relation:

$$\prod_{i=1}^N a_i^{\Delta_{ji}} = I \quad \forall i = 1, \dots, N \quad (2.8)$$

the order of \mathcal{G} , denoted as $|\mathcal{G}|$, is equal to the number of recurrent configurations. This is a consequence of the fact that if C and C' are any two recurrent configurations, then there is an element $g \in \mathcal{G}$ such that $C' = gC$. We thus have:

$$|\mathcal{G}| = |\mathbf{R}| \quad (2.9)$$

2.3 The evolution operator and the steady state

We consider a vector space \mathcal{V} whose basis vectors are the different configurations of \mathbf{R} . The state of the system at time t will be given by a vector

$$|P(t)\rangle = \sum_C \text{Prob}(C, t) |C\rangle , \quad (2.10)$$

where $\text{Prob}(C, t)$ is the probability that the system is in the configuration C at time t . The operators a_i can be defined to act on the vector space \mathcal{V} through their operation on the basis vectors.

The time evolution is Markovian, and governed by the equation

$$|P(t+1)\rangle = \mathcal{W} |P(t)\rangle \quad (2.11)$$

where

$$\mathcal{W} = \sum_{i=1}^N p_i a_i \quad (2.12)$$

To solve the time evolution in general, we have to diagonalize the evolution operator \mathcal{W} . Being mutually commuting, the a_i may be simultaneously diagonalized, and this also diagonalizes \mathcal{W} . Let $|\{\phi\}\rangle$ be the simultaneous eigenvector of $\{a_i\}$, with eigenvalues $\{e^{i\phi_i}\}$, for $i = 1, \dots, N$. Then

$$a_i |\{\phi\}\rangle = e^{i\phi_i} |\{\phi\}\rangle \quad \forall i = 1, \dots, N. \quad (2.13)$$

We recall that the a operators now satisfy the relation (2.8). Applying the l.h.s. of this relation to the eigenvector $|\{\phi\}\rangle$ gives $\exp(i \sum_j \Delta_{kj} \phi_j) = 1$, for every k , so that $\sum_j \Delta_{kj} \phi_j = 2\pi m_k$, or inverting,

$$\phi_j = 2\pi \sum_k [\Delta^{-1}]_{jk} m_k , \quad (2.14)$$

where Δ^{-1} is the inverse of Δ , and the m_k 's are arbitrary integers.

The particular eigenstate $|\{0\}\rangle$ ($\phi_j = 0$ for all j) is invariant under the action of all the a 's, $a_i |\{0\}\rangle = |\{0\}\rangle$. Thus $|\{0\}\rangle$ must be the stationary state of the system since

$$\sum_i p_i a_i |\{0\}\rangle = \sum_i p_i |\{0\}\rangle = |\{0\}\rangle . \quad (2.15)$$

We now see explicitly that the steady state is independent of the values of the p_i 's and that *in the steady state, all recurrent configurations occur with equal probability.*

2.4 Recurrent and transient configurations

Given a stable configuration of the sandpile, how can we distinguish between transient and recurrent configurations? A first observation is that there are some forbidden subconfiguration that can never be created by addition of sand and relaxation, if not already present in the initial state. The simplest example on the square lattice case is a configuration of two adjacent sites of height 0, $\boxed{0 \mid 0}$. Since $z_i \geq 0$, a site of height 0 can only be created as a result of toppling at one of the two sites (toppling from anywhere else can only increase his height). But a toppling of either of this sites results in a height of at least 1 in the other. Thus any configuration which contains two adjacent 0's is transient. With the same argument is easy to prove that the following configurations can never appear in a recurrent configuration:

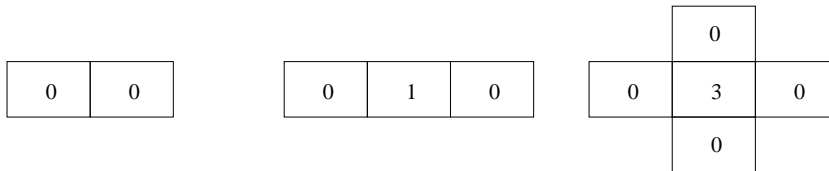


Figure 2.3 Examples of forbidden subconfigurations

In general a forbidden subconfiguration (FSC) is a set F of r sites ($r \geq 1$), such that the height z_j of each site j in F is less of the number of neighbors of j in F , precisely:

$$z_i < \sum_{j \in F \setminus \{i\}} (-\Delta_{ij}) \quad \forall i \in F \quad (2.16)$$

The proof of this assertion is by induction on the number of sites in F . For example the creation of the $\boxed{0 \mid 1 \mid 0}$ subconfiguration must involve toppling at one of end sites, but then the subconfiguration must have had a $\boxed{0 \mid 0}$ before the toppling, and this was shown before to be forbidden.

An interesting consequence of the existence of forbidden configurations is the following: consider an ASM on an undirected graph, with N_b bonds between sites, then in any recurrent configuration the number of sandgrains is greater or equal to N_b . Note that here we do not count the boundary bonds, corresponding to particles leaving the system. To prove this, we note that if the inequality is not true for any configuration, it must have a FSC in it.

2.4.1 The multiplication by identity test

A more systematic way to test the recurrence of a given configuration could be found by using some operator properties of the a_i (2.7). Let us take the example of a sandpile defined on an $N \times N$ square lattice. Multiplying all the relations (2.7)

gives

$$\prod_i a_i^4 = \prod_i a_i^{n_i}, \quad (2.17)$$

where n_i is the number of neighbors of a given site i , i.e. 4 for a bulk site, 2 or 3 for a boundary site. Now we can use the property for the a_i that on the set R of recurrent configurations the inverses are defined, and this yields to

$$\prod_i a_i^{4-n_i} = 1. \quad (2.18)$$

So, to check whether a configuration C is recurrent, one has to add a particle at each boundary site (two on corner sites), relax the system, and then check whether the final configuration is the same as C , in which case the configuration is recurrent. In the next section we will see how to obtain the same result in an easier and faster way.

2.4.2 Burning test

There is a simple recursive procedure to discover if a configuration is recurrent. We consider a test set, say T , of sites. In the beginning T consists of all the sites of the lattice we are considering; we first test the hypothesis that T is a FSC using the inequalities (2.16). If these inequalities are satisfied for all sites in T , then the hypothesis is true and the configuration in exam is transient. Otherwise there are some sites for which the inequalities are violated, these sites cannot be part of any FSC, in fact the inequalities will remain unsatisfied even though T is replaced by a smaller subset of sites. We can now delete them from T to obtain a new subset T' , we say we “burn” these sites and the remaining are “unburnt”; at this point it is possible to check whether T' is a FSC with the previous procedure. We continue following this scheme until we cannot burn anymore site. If we get a finite subset F of unburnt sites this is a FSC and the configuration is transient, if the set of unburnt sites becomes empty the configuration in exam is found to be recurrent. We call the procedure just presented the *burning test*.

In the *burning test* it does not matter in which order the sites are burnt. It is however useful to introduce the concept of time of burning and to add to the graph a site, named *sink*, which is connected to all the “boundary” sites with as many links as the number of lost particles in a toppling by the boundary sites in exam, it never topples and only collects sand. There is a natural way to choose a time of burning for each site. At time $t = 0$, all the sites in T are unburnt except the sink. At any time a site is called “burnable” iff the inequality (2.16) is unsatisfied with respect to the set $T^{(t)}$ reached at that time, then a burnable site at time t becomes burnt at time $t + 1$, and so remains for the next times. With this prescription we label each site of the graph with a burning time, depending just on the configuration in exam.

Take now an arbitrary site i , except the sink. Let $\tau_i + 1$ be the time step at which this is burnt, then the burning rule implies that at time τ_i at least one of his

neighbor sites has been burnt. Let r_i be the number of such neighbors and let us write:

$$\xi_i = \sum'_j (-\Delta_{ij}) \quad (2.19)$$

where the primed summation runs over all unburnt neighbors of i at time τ_i . Then we have $z_i \geq \xi_i$ since the site i is burnable at time τ_i ; but, since it was not burnable at time $\tau_i - 1$ we must also have:

$$z_i < \xi_i + K \quad (2.20)$$

where K is the number of bonds linking i to his neighbors which were unburnt at time τ_i . During the burning test we say that fire reaches the site i by one of the K bonds. Obviously when $K = 1$ there is just one possibility so there are no problems, and we say that the fire reaches i from the only site possible. If $K > 1$ we have to select one bond through which the fire reaches i depending on his height z_i . For this purpose we order the bonds converging on the site i in some sequence (e.g. $\{(i, i_1), (i, i_2), (i, i_3), \dots\}$), the order is arbitrary and can be chosen independently on each site i . Now we can write $z_i = \xi_i + s - 1$ for some $s > 0$, we say that fire reaches i using the s -th link in the ordered list of the possible ones. With this procedure we have got a unique path for the fire to reach each site i , given the configuration of heights in the sandpile and the prescription on the order of bonds converging on each site. The set of bonds along which fire propagates, connects the sink with each site in the graph, and there are no loops in each path. Thus the set just obtained is a spanning tree on the graph $G' = G + \{sink\}$.

So choosing a particular prescription for a given graph we can obtain by each configuration a unique spanning tree. For example on a square lattice we have four bonds for each site, let us call them N-E-S-W, where the cardinal points denotes the direction of incidence, we can choose the prescription N>E>S>W and obtain for a recurrent configuration the corresponding spanning tree. In (fig. 2.4) is shown a burning test for a 4×4 square lattice, with prescription NESW, with \blacksquare are denoted the sites such that, connected together, represent the sink, with \bullet the sites burnt at the given time of each step of the algorithm and with \cdots , the bonds through which the fire could have reached the site but were rejected.

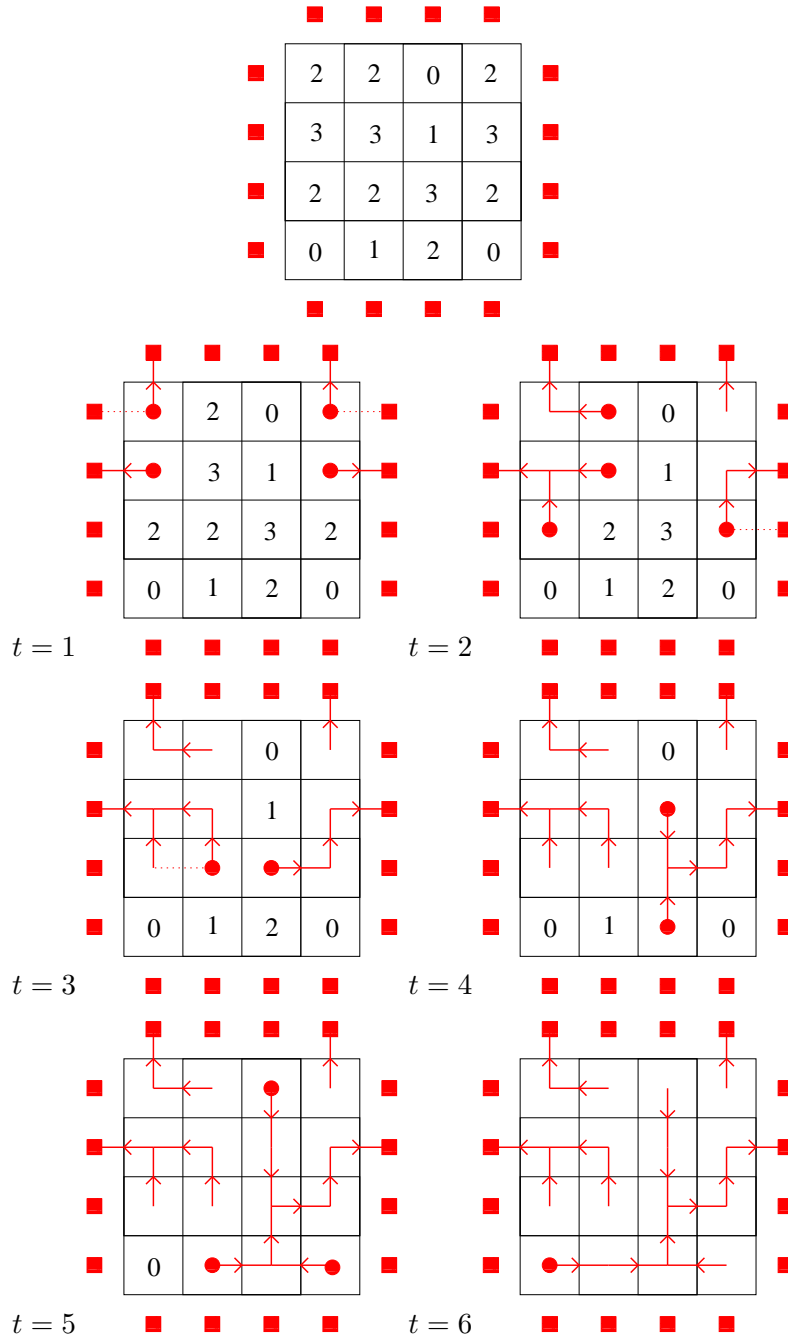


Figure 2.4 Example of burning test acting on a given configuration, at each time is displayed the progress in the algorithm until at $t=6$ all sites become “burnt”

2.5 Algebraic aspects

We want to report some features of the abelian group \mathcal{G} associated to the ASM. In particular we determine scalar function, invariant under toppling, and the rank of the group for the square lattice.

Furthermore we recall that any finite abelian group \mathcal{G} can be expressed as a product of cyclic groups in the following form:

$$\mathcal{G} \cong \mathbf{Z}_{d_1} \times \mathbf{Z}_{d_2} \times \cdots \times \mathbf{Z}_{d_g} \quad (2.21)$$

That is, the group is isomorphic to the direct product of g cyclic groups of order d_1, d_2, \dots, d_g . Moreover the integers $d_1 \geq d_2 \geq \dots \geq d_g > 1$ can be chosen such that d_i is an integer multiple of d_{i+1} and, under this condition, the decomposition is unique. In the following we determine the canonical decomposition of the group.

2.5.1 Toppling invariants

The space of all configurations $\{z_i\}$ (with $z_i \geq 0$) constitutes a commutative semigroup over the vertex-set of the ambient graph, with the addition between configurations defined as a sitewise addition of heights with relaxation, if necessary. We define an equivalency relation on this semigroup by saying that two configurations $\{z_i\}$ and $\{z'_i\}$ are equivalent iff there exists $|V|$ integers $n_j, j = 1, \dots, N$, such that:

$$z'_i = z_i - \sum_j \Delta_{ij} n_j \quad \forall i \in V \quad (2.22)$$

This equivalence is said “equivalence under toppling”, and each equivalence class with respect to (2.22) contains one and only one recurrent configuration. One can associate to each configuration $\{z_i\}$ a recurrent configuration C defining:

$$C[z_i] = \prod_i a_i^{z_i} C^* \quad (2.23)$$

where C^* is a given recurrent configuration. If $\{z_i\}$ and $\{z'_i\}$ are in the same equivalence class, then $C[z_i] = C[z'_i]$, indeed we have that:

$$\begin{aligned} C[z'_i] &= \prod_i a_i^{z_i - \sum_j \Delta_{ij} n_j} C^* = \left(\prod_i a_i^{z_i} \right) \left(\prod_{ij} a_i^{\Delta_{ij} n_j} \right) C^* \\ &= \left(\prod_i a_i^{z_i} \right) \left(\prod_j \left(\prod_i a_i^{\Delta_{ij} n_j} \right) \right) C^* = \prod_i a_i^{z_i} C^* = C[z_i]. \end{aligned} \quad (2.24)$$

Using the (2.22) two stable configurations can be equivalent under toppling.

Toppling invariants are scalar functions defined on the space of all the configurations of the sandpile, such that their value is the same for configurations that are equivalent under toppling. Given the toppling matrix Δ for an N sites sandpile, we define N rational functions $Q_i, i \in \{1, \dots, N\}$, as follows

$$Q_i(\{z_j\}) = \sum_j \Delta_{ij}^{-1} z_j \pmod{1} \quad (2.25)$$

It is straightforward to prove that the functions Q_i are toppling invariants, indeed the toppling at site k changes $C \equiv \{z_i\} \rightarrow C' \equiv \{z_i - \Delta_{ik}\}$, and the linearity of the Q_i 's in the height variables permits to write:

$$Q_i(C') = Q_i(C) - \sum_j \Delta_{ij}^{-1} \Delta_{jk} = Q_i(C) \pmod{1} \quad (2.26)$$

These functions are rational-valued but they can be made integer-valued by multiplication upon an adequate integer. So these functions can be used to label the recurrent configurations. Thus the space of recurrent configurations can be replaced by the set of N -uples (Q_1, Q_2, \dots, Q_N) , but this labelling is generally overcomplete, they being not all independent.

It is desirable to isolate a minimal set of invariants, and this can be done for an arbitrary ASM using the classical theory of Smith normal form for integer matrices [22].

Any nonsingular $N \times N$ integer matrix Δ can be written in the form:

$$\Delta = ADB \quad (2.27)$$

where A and B are $N \times N$ integer matrices with determinant ± 1 , and D is a diagonal matrix

$$D_{ij} = d_i \delta_{ij} \quad (2.28)$$

where the eigenvalues d_i are defined as follows:

1. d_i is a multiple of d_{i+1} for all $i = 1$ to $N - 1$
2. $d_i = e_{i-1}/e_i$ where e_i stands for the greatest common divisor of the determinants of all the $(N - i) \times (N - i)$ submatrices of Δ (note that $e_N = 1$)

The matrix D is uniquely determined by Δ but the matrices A and B are far from unique. The d_i are called the *elementary divisors* of Δ .

In terms of the decomposition (2.27), we define the set of scalar functions $I_i(C)$ by

$$I_i(C) = \sum_j (A^{-1})_{ij} z_j \pmod{d_i} \quad (2.29)$$

Due to the unimodularity of A (fact that guarantees the existence of an integer inverse matrix for A), these functions are integer-valued, and are toppling invariant, explicetely, given the equivalence under toppling relation (2.22), we have:

$$I_i[z'_j] = \sum_j (A^{-1})_{ij} z_j - \sum_{jk} (A^{-1})_{ij} \Delta_{jk} n_k \quad (2.30)$$

$$= I_i[z_j] - \sum_{jklm} (A^{-1})_{ij} A_{j\ell} D_{\ell m} B_{mk} n_k = \quad (2.31)$$

$$= I_i[z_j] - \sum_{jk} D_{ij} B_{jk} n_k \quad (2.32)$$

$$= I_i[z_j] - d_i \sum_k B_{ik} n_k = I_i[z_j] \pmod{d_i} \quad (2.33)$$

Only the I_i for which $d_i \neq 1$ are nontrivial, and we note that these invariants are far from unique, because they are defined in terms of A which is not unique itself. The I_i 's can also be written in terms of the Q_i 's as follows:

$$I_i[C] = \sum_j d_i B_{ij} Q_j[C] \quad (2.34)$$

We now show that the set of nontrivial invariants is always minimal and complete. Let g be the number of $d_i > 1$, we associate at each recurrent configuration a g -uple (I_1, I_2, \dots, I_g) where $0 \leq I_i < d_i$. The total number of distinct g -uples is $\prod_{i=1}^g d_i = |\mathcal{G}|$.

We first show that this mapping from the set of recurrent configurations to g -uples is one-to-one. Let us define operators e_i by the equation

$$e_i = \prod_{j=1}^N a_j^{A_{ji}} \quad 1 \leq i \leq g \quad (2.35)$$

Acting on a fixed configuration $C^* = \{z_j\}$, e_i yields a new configuration, equivalent under toppling to the configuration $\{z_j + A_{ji}\}$. If the g -uple corresponding to C^* is $(I_1^*, I_2^*, \dots, I_g^*)$, from (2.29) it follows that $e_i C^*$ has toppling invariants $I_k = I_k^* + \delta_{ik}$. By operating with these operators $\{e_i\}$ sufficiently many times on C^* , all $|\mathcal{G}|$ values for the g -uple (I_1, I_2, \dots, I_g) are obtainable. Thus there is at least one recurrent configuration corresponding to any g -uple (I_1, I_2, \dots, I_g) . As the total number of recurrent configurations equals the number of g -uples (2.9), we see that there is a one-to-one correspondence between the g -uples (I_1, I_2, \dots, I_g) and the recurrent configurations of the ASM.

To express the operators a_j in terms of e_i , we need to invert the transformation (2.35). This is easily seen to be:

$$a_j = \prod_{i=1}^g e_i^{(A^{-1})_{ij}} \quad 1 \leq j \leq N \quad (2.36)$$

Thus the operators e_i generate the whole of \mathcal{G} . Since e_i acting on a configuration increases I_i by one, leaving the other invariants unchanged, and since I_i is only defined modulo d_i , we see that

$$e_i^{d_i} = I \quad \text{for } i = 1 \text{ to } g \quad (2.37)$$

Note that the definition (2.35) makes sense for i between $g+1$ and N , and implies relations among the a_j operators.

This shows that \mathcal{G} has a canonical decomposition as a product of cyclic groups as in (2.21), with d_i 's defined in (2.28). We thus have shown that the generators and the group structure of \mathcal{G} can be entirely determined from its toppling matrix Δ , through its normal decomposition (2.27).

The invariants $\{I_i\}$ also provide a simple additive representation of the group \mathcal{G} . We define a binary operation of "addition" (denoted by \oplus) on the space of

recurrent configurations by adding heights sitewise, and then allowing the resulting configuration to relax. From the linearity of the I_i 's in the height variables, and their invariance under toppling, it is clear that under this addition of configurations, the I_i 's also simply add. Thus for any recurrent configurations C_1 and C_2 one has

$$I_i(C_1 \oplus C_2) = I_i(C_1) + I_i(C_2) \pmod{d_i} \quad (2.38)$$

The I_i 's provide a complete labelling of \mathbf{R} . There is a unique recurrent configuration, denoted by C_{id} , for which all $I_i(C_{id})$ are zero. Also, each recurrent C has a unique inverse $-C$, also recurrent, and determined by $I_i(-C) = -I_i(C) \pmod{d_i}$. Therefore the addition \oplus is a group law on \mathbf{R} , with identity given by C_{id} . M. Creutz first gave an algorithm to compute this configuration in [18].

There is a one-to-one correspondence between recurrent configurations of ASM and elements of the group \mathcal{G} : we associate to the group element $g \in \mathcal{G}$, the recurrent configuration gC_{id} , and from (2.38) follows that for all $g, g' \in \mathcal{G}$

$$gC_{id} \oplus g'C_{id} = (gg')C_{id} \quad (2.39)$$

Thus the set of recurrent configurations with the operation \oplus form a group which is isomorphic to the multiplicative group \mathcal{G} , result first proved in [18]. The invariants $\{I_i\}$ provide a simple labelling of the recurrent configurations. Since a recurrent configuration can also be uniquely determined by its height variables $\{z_i\}$, the existence of forbidden configuration (2.16) in ASM's implies that this heights satisfy many inequality constraints.

2.5.2 Rank of \mathcal{G} for a rectangular lattice

For a general toppling matrix Δ , it is difficult to say much more about the group structure of \mathcal{G} . To obtain some useful results we now consider the toppling matrix Δ of a finite $L_1 \times L_2$ 2-dimensional square lattice. In this framework is more convenient to label the sites not by a single index i running from 1 to $N = L_1 L_2$, but by two Cartesian coordinates (x, y) , with $1 \leq x \leq L_1$ and $1 \leq y \leq L_2$. The toppling matrix is the discrete Laplacian as defined in (2.3), given by $\Delta(x, y; x, y) = 4$, $\Delta(x, y; x', y') = -1$ if the sites are nearest-neighbors (i.e. $|x - x'| + |y - y'| = 1$), and zero otherwise. We assume, without loss of generality, that $L_1 \geq L_2$. The relations (2.6) satisfied by operators $a(x, y)$, using the fact that the operators has an inverse on \mathbf{R} , can be rewritten in the form

$$a(x+1, y) = a^4(x, y) a^{-1}(x, y+1) a^{-1}(x, y-1) a^{-1}(x-1, y) \quad (2.40)$$

where we adopt the convention that

$$a(x, 0) = a(x, L_2 + 1) = a(0, y) = a(L_1 + 1, y) = I \quad \forall x, y \quad (2.41)$$

The equations (2.40) can be recursively solved to express any operator $a(x, y)$ as a product of powers of $a(1, y)$. Therefore the group \mathcal{G} can be generated by the L_2

operators $a(1, y)$. Denoting the rank of \mathcal{G} (minimal number of generators) by g , this implies that

$$g \leq L_2 \quad (2.42)$$

In the special case of a linear chain, $L_2 = 1$, we see that $g = 1$, and thus \mathcal{G} is cyclic. Equations (2.40) permits also to express $a(L_1 + 1, y)$ in term of powers of $a(1, y)$ say

$$a(L_1 + 1, y) = \prod_{y'} a(1, y')^{n_{yy'}} \quad (2.43)$$

where the $n_{yy'}$ are integers which depend on L_1 and L_2 and which can be eventually determined by solving the linear recurrence relation (2.40). The condition (2.41), $a(L_1 + 1, y) = I$ then leads to the closure relations

$$\prod_{y'}^{L_2} a(1, y')^{n_{yy'}} = I \quad \forall y = 1, \dots, L_2 \quad (2.44)$$

The equations (2.44) give a presentation of \mathcal{G} , the structure of which can be determined from the normal form decomposition of the $L_2 \times L_2$ integer matrix $n_{yy'}$. This is considerably easier to handle than the normal form decomposition of the much larger matrix Δ needed for an arbitrary ASM. Even though this is a real computational improvement, the calculation for arbitrary L_1 is not trivial.

In the particular case of square-shaped lattice, where $L_1 = L_2 = L$, using the above algorithm is possible to find the structure of \mathcal{G} , and to prove that for an $L \times L$ square lattice we have

$$g = L \quad \text{for} \quad L_1 = L_2 = L \quad (2.45)$$

3. Cluster-toppling rules and exotic operators

In this chapter we present a generalization of the toppling rule which preserves the group properties of the model, and has some interesting involvements with the identification of recurrent configurations. Then we propose a class of operators N_i that have some particular exchange properties, although being in a non-abelian extension of the original ASM algebra. We also show the possibility of obtaining a particular stationary state by the repeated action of the operators N_i on a given state, we study this stationary state and we find a close relation with the above mentioned cluster-toppling rules. We study in more detail portions of the square lattice of various particular shapes.

3.1 Generalized toppling rules

In chapter 2, we introduced the two basic rules of the ASM: the “addition rule” and the “toppling rule”. The addition rule has a general formulation, and, in the identification of a Markov Chain, it is flexible because of the possibility to make different choices for the rates p_i , at which particles are added on each site. On the other hand the toppling rule is maybe not the most general. Indeed a toppling rule took the form of a single-variable check, labelled by a site index i , $z_i < \bar{z}_i$ which, if failing causes an “instability” in the height profile, which relaxes with a constant shift $z_j \rightarrow z_j - \Delta_{ij}$ such that the total mass can only decrease, with some conditions that ensure both the finitness of the relaxation process, and the fact that the result has no ambiguity in the case of multiple violated disequalities at some intermediate steps.

Theorem 1. *Given an ASM on a graph $G = (E, V)$ and a toppling matrix Δ , if \tilde{C} is unstable, consider the set S of sequences $(i_1, \dots, i_{N(s)})$ such that $t_{i_{N(s)}} \dots t_{i_2} t_{i_1} \tilde{C}$ is a valid sequence of topplings, and produces a stable configuration $C(s)$, some facts are true:*

- (0) S is non-empty;
- (1) $C(s) = C(s')$ for each $s, s' \in S$, i.e. the final stable configuration does not depend upon possible choices of who topples when;

$$(2) N(s) = N(s') = N(\tilde{C}) \quad \forall s, s' \in S$$

$$(3) \forall s, s' \in S \quad \exists \pi \in \mathcal{S}_{N(s)} : i_\alpha^{(s)} = i_{\pi(\alpha)}^{(s')} \text{ for } \alpha = 1, \dots, N(\tilde{C}), \text{ i.e. the toppling sequences differ only by a permutation.}$$

Proof. Here we prove (3), given (1) and (0). As a restatement of (3), we have that one can define a vector $\vec{n}(\tilde{C}) \in \mathbb{N}^{|V|}$ as the number of occurrence of each site in any of the sequence of S . Then, we have that the final configuration is

$$C = \tilde{C} + \Delta \cdot \vec{n} \quad (3.1)$$

The fact that \vec{n} is unique is trivially proven. Indeed, as S is non-empty, we have a first candidate \vec{n}_0 , and thus a solution of the non-homogeneous linear system (in \vec{n})

$$\Delta \cdot \vec{n} = C - \tilde{C}.$$

If there was another solution \vec{n}_1 , then we would have that $\vec{n}' = \vec{n}_1 - \vec{n}_0$ is a solution of the homogeneous system

$$\Delta \cdot \vec{n}' = \vec{0}.$$

But Δ is a square matrix of the form Laplacian+mass, such that the spectrum is all positive (we saw how it is a strictly-dissipative diffusion kernel), so it can not have non-zero vectors in its kernel. This proves the uniqueness of \vec{n} , i.e. (3). But (3) is stronger than (2), and the fact that $C = \tilde{C} + \Delta \cdot \vec{n}$ also implies (1). So the theorem is proven. \square

The standard toppling rule can be shortly rewritten as:

$$\text{if } z_i \geq \bar{z}_i = \Delta_{ii} \implies z_j \rightarrow z_j + \Delta_{ij} \quad \forall j \quad (3.2)$$

Pictorially, on a square lattice, we can draw the heights at a given site i and at its nearest-neighbors i_1, i_2, i_3, i_4 as

$$\begin{array}{|c|c|c|} \hline & z_{i_1} & \\ \hline z_{i_4} & z_i & z_{i_2} \\ \hline & z_{i_3} & \\ \hline \end{array} \quad (3.3)$$

and an example of typical toppling is

$$\begin{array}{|c|c|c|} \hline 0 & 4 & 0 \\ \hline 0 & 4 & 0 \\ \hline 0 & & \\ \hline \end{array} \longrightarrow \begin{array}{|c|c|c|} \hline & 1 & \\ \hline 1 & 0 & 1 \\ \hline & 1 & \\ \hline \end{array} \quad (3.4)$$

where the initial value of z_i is equal to $\bar{z}_i = 4$, so it is the only site that becomes unstable and requires the toppling shown in figure.

A straightforward generalization of this prescription is to consider a site stable or unstable not just for “ultra-local” (i.e. single-site) properties (like the overcoming of the site threshold) but also for local properties that depend on the heights

at more than one sites. Similarly, we would have toppling rules $\vec{\Delta}_\alpha = \{\Delta_{\alpha j}\}_{j \in V}$ with more than a single positive entry. Still we want to preserve the “exchange” properties of toppling procedures which led to the abelianity of the *drop* operators a_i , and this could be in principle such a severe constraint that we could not find essentially any new possibility. As we show now, by direct construction, this is *not* the case. We can define some *cluster-toppling* rules, labelled by whole subsets $I \subseteq V$ of the set of sites, instead that by a single site, and for any subset I introduce the toppling rule

$$\text{if } \forall i \in I \quad z_i \geq \sum_{\alpha \in I} \Delta_{i\alpha} \quad \Longrightarrow \quad z_k \rightarrow z_k - \sum_{\alpha \in I} \Delta_{\alpha k} \quad \forall k \quad (3.5)$$

These rules clearly define some sandpile model, that, under some constraints on the choice of toppling clusters $\mathcal{L} = \{I\}$, we will prove later to be abelian. But, before this, we address the simpler issue of cheking for the finiteness of the space of configurations. It is trivial to see that if, for any site i , there is no set $\{i\} \in \mathcal{L}$, but only an arbitrary number of “large” clusters $I \in \mathcal{L}$, $|I| \geq 2$, $i \in I$, then all the configurations of height

$$z_i = n \in \mathbb{N}, \quad z_j = 0 \quad j \neq i \quad (3.6)$$

are allowed and stable, thus a necessary condition for having a finite set of stable configurations is

$$\{i\} \in \mathcal{L} \quad \forall i \in V \quad (3.7)$$

this is also sufficient, as even in the standard ASM we have a number $\prod \bar{z}_i$ of stable configurations (where \bar{z}_i is the source of instability for each site), and this number can only decrease when adding new toppling rules.

We define \mathcal{L}_{std} the set of toppling cluster for the standard toppling rules, that is

$$\mathcal{L}_{std} = \{\{i\}_{i \in V}\} \quad (3.8)$$

So we ask wether a given set \mathcal{L} of cluster-toppling give rise to a finite abelian sandpile. Say $I_{(1)}$ and $I_{(2)}$ are two clusters in \mathcal{L}

Theorem 2. *Given an ASM on a graph $G = (E, V)$, with a symmetric toppling matrix Δ , $\{\vec{\Delta}_I\}_{I \in \mathcal{L}}$ and $\mathcal{L} \supseteq \mathcal{L}_{std}$. A necessary and sufficient condition for the sandpile to be abelian is that*

$$\text{each component of } I_{(1)} \setminus I_{(2)} \in \mathcal{L} \quad \forall I_{(1)}, I_{(2)} \in \mathcal{L} \quad (3.9)$$

Proof. Let us call $J = I_{(1)} \cap I_{(2)}$, then there are two cases:

- (a) $J = \emptyset$
- (b) $J \neq \emptyset$

In case **a** the compatibility is obvious, indeed if we make the toppling for $I_{(1)}$ then the heights in $I_{(2)}$ can only increase for the properties of the toppling matrix Δ . After the topplings also of the sites in $I_{(2)}$ have been done, the final height configuration will be

$$z'_k = z_k - \sum_{i \in I_{(1)}} \Delta_{ik} - \sum_{j \in I_{(2)}} \Delta_{jk} \quad (3.10)$$

this expression is clearly symmetric under the exchange of $I_{(1)}$ and $I_{(2)}$.

In case **b** we shortly recall the toppling rule for $I_{(1)}$ and $I_{(2)}$ (3.5)

$$\text{if } \forall i \in I_{(1)} \quad z_i \geq \sum_{\alpha \in I_{(1)}} \Delta_{i\alpha} \implies z_k \rightarrow z_k - \sum_{\alpha \in I_{(1)}} \Delta_{\alpha k} \quad \forall k \quad (3.11a)$$

$$\text{if } \forall i \in I_{(2)} \quad z_i \geq \sum_{\alpha \in I_{(2)}} \Delta_{i\alpha} \implies z_k \rightarrow z_k - \sum_{\alpha \in I_{(2)}} \Delta_{\alpha k} \quad \forall k \quad (3.11b)$$

now we note that we can split the sums in the contribution from J and the one from the remaining sites of each subset

$$\sum_{\alpha \in I_{(1)}} = \sum_{\alpha \in I_{(1)} \setminus J} + \sum_{\alpha \in J}$$

$$\sum_{\alpha \in I_{(2)}} = \sum_{\alpha \in I_{(2)} \setminus J} + \sum_{\alpha \in J}$$

Now we can topple first $I_{(1)}$ and so update the configuration $\{z_i\} \rightarrow \{z'_i\}$ as follows

$$z'_i = z_i + \sum_{\alpha \in I_{(1)} \setminus J} \Delta_{\alpha i} + \sum_{\alpha \in J} \Delta_{\alpha i} \quad \forall i \in V$$

At this point, for the updated configuration the following relations are valid

$$\forall i \in I_{(2)} \setminus J \quad z'_i = z_i - \sum_{\alpha \in I_{(1)} \setminus J} \Delta_{\alpha i} - \sum_{\alpha \in J} \Delta_{\alpha i} \geq \quad (3.12a)$$

$$\geq \sum_{\alpha \in I_{(2)} \setminus J} \Delta_{i\alpha} + \sum_{\alpha \in J} \Delta_{i\alpha} - \sum_{\alpha \in I_{(1)} \setminus J} \Delta_{\alpha i} - \sum_{\alpha \in J} \Delta_{\alpha i} \geq \quad (3.12b)$$

$$\geq \sum_{\alpha \in I_{(2)} \setminus J} \Delta_{i\alpha} - \sum_{\alpha \in I_{(1)} \setminus J} \Delta_{\alpha i} \geq \quad (3.12c)$$

$$\geq \sum_{\alpha \in I_{(2)} \setminus J} \Delta_{i\alpha} \quad (3.12d)$$

in line (3.12b) we used the symmetry property of the toppling matrix to cancel out the second and the fourth terms, in line (3.12c) we used the property the off-diagonal elements Δ_{ij} to be negative or equal to zero to obtain the inequality in the last line, indeed if $A > B$, if $c_i \geq 0$ then $A + \sum c_i > B$ a *fortiori*.

In the case it does not exist the toppling rule for $I_{(2)} \setminus J$, there exists a configuration of heights (the minimal heights such that both $I_{(1)}$ and $I_{(2)}$ are unstable) such that toppling first $I_{(1)}$ or $I_{(2)}$ leads immediately after a single toppling to two distinct stable configurations, so we see that necessary part of the theorem holds. As a consequence, as $\mathcal{L} \supseteq \mathcal{L}_{std}$, given $I \in \mathcal{L}$ we have that all the $I' \subseteq I$ are in \mathcal{L} , and thus all of its components. In particular disconnected I 's are simply redundant, and we can restrict \mathcal{L} to contain only connected clusters without loss of generality.

Conversely, if $I_{(2)} \setminus J \in \mathcal{L}$ (and $I_{(1)} \setminus J \in \mathcal{L}$ by symmetry), in the two “histories” in which we toppled $I_{(1)}$ or $I_{(2)}$, we can still topple $I_{(2)} \setminus J \in \mathcal{L}$ and $I_{(1)} \setminus J \in \mathcal{L}$ respectively and put them back on the same track, i.e.

$$t_{I_{(1)} \setminus J} t_{I_{(2)}} \equiv t_{I_{(2)} \setminus J} t_{I_{(1)}} \quad (3.13)$$

as operators when applied to configurations C such that both $I_{(1)}$ and $I_{(2)}$ are unstable. \square

We want also to produce a proof similar to that for standard toppling rule in theorem 1 for the cluster-toppling ASM.

We have $G = (E, V)$, and the induced toppling matrix Δ , and a set \mathcal{L} of connected subsets of V , with $\mathcal{L} \supseteq \mathcal{L}_{std} = \{\{i\}_{i \in V}\}$. Call $\vec{\Delta}_i = \{\Delta_{ij}\}_{j \in V}$, and $\vec{\Delta}_I = \sum_{i \in I} \vec{\Delta}_i$. A toppling t_I changes \vec{z} into $\vec{z} - \vec{\Delta}_I$.

Theorem 3. *If \tilde{C} is unstable, consider the set S of sequences $s = (I_1, \dots, I_{N(s)})$ such that $t_{I_{N(s)}} \dots t_{I_2} t_{I_1} \tilde{C}$ is a valid sequence of topplings and produces a stable configuration $C(s)$. Some facts are true:*

- (0) S is non-empty;
- (1) $C(s) = C(s') \quad \forall s, s' \in S$;
- (2) $\sum_{\alpha=1}^{N(s)} |I_{\alpha}^{(s)}| = \sum_{\alpha=1}^{N(s')} |I_{\alpha}^{(s')}| \quad \forall s, s' \in S$;
- (3) defining $\vec{\chi}_I = \begin{cases} 1 & i \in I \\ 0 & i \notin I \end{cases}$, $\sum_{\alpha=1}^{N(s)} \vec{\chi}_{I_{\alpha}^{(s)}}$ is the same for all the sequences and is some vector $\vec{n}(\tilde{C})$

Proof. (of (3) and (2) given (1) and (0)) Again, the final stable configuration is $C = \tilde{C} + \Delta \cdot \vec{n}$, and the uniqueness of \vec{n} is proven along the same line as the proof for standard ASM. Then, as (3) is a strenghtening of (2), the theorem is proven. remark however some qualitative difference with the simplest case of ordinary ASM: it can well be that $N(s) \neq N(s')$, and s and s' do not differ simply by a permutation (e.g., in the relaxation of $\begin{bmatrix} 3 & 4 & 3 \end{bmatrix}$ by $t_3 t_{12}$ or by $t_1 t_3 t_2$), and analogously the kernel

$$\sum_j n_I \vec{\Delta}_{Ij} = 0 \quad \forall I \in \mathcal{L}$$

is non-empty for $\mathcal{L} \supseteq \mathcal{L}_{std}$, as Δ is rectangular (e.g. $n_{12} = a$, $n_1 = n_2 = -a$, $n_I = 0$ otherwise is a null vector of Δ). Only in the “basis” of \mathcal{L}_{std} we have a unique solution, and of course the versor \hat{e}_I , in $\mathbb{Z}^{|\mathcal{L}|}$, reads $\vec{\chi}_I$ in this basis. \square

We present for clarity the case in which the rule is defined for all the 2-clusters, dimers. In this case we have

$$\mathcal{L} = \{\{i, j\}_{ij \in E}\} \cup \{\{i\}_{i \in V}\}, \quad (3.14)$$

and the general rule (3.5) becomes:

$$\text{if } \begin{cases} ij \in E \\ z_i \geq \Delta_{ii} + \Delta_{ij} \\ z_j \geq \Delta_{jj} + \Delta_{ij} \end{cases} \implies z_k \rightarrow z_k - \Delta_{ik} - \Delta_{jk} \quad \forall k, \quad (3.15)$$

we can now pictorially draw on a square lattice the heights for a given cluster, formed by the sites i and j , and its nearest-neighbors $i_1, i_2, i_3, j_1, j_2, j_3$ as

$$\begin{array}{|c|c|c|} \hline & z_{i_1} & z_{j_1} \\ \hline z_{i_3} & z_i & z_j & z_{j_2} \\ \hline & z_{i_2} & z_{j_3} \\ \hline \end{array} \quad (3.16)$$

so a typical 2-cluster toppling is:

$$\begin{array}{|c|c|c|c|} \hline & 0 & 0 & \\ \hline 0 & 3 & 3 & 0 \\ \hline & 0 & 0 & \\ \hline \end{array} \longrightarrow \begin{array}{|c|c|c|c|} \hline & 1 & 1 & \\ \hline 1 & 0 & 0 & 1 \\ \hline & 1 & 1 & \\ \hline \end{array} \quad (3.17)$$

in which in the initial state both the sites i and j have height equal to $\bar{z}_i - 1 = 3$ and become unstable with respect to the (3.15), it is therefore necessary to topple the sites obtaining the final configuration. We note that doing a single cluster-toppling is the same as making two consecutive normal topplings, at condition that we permit negative height in the intermediate steps and force the toppling also in the case it is not necessary ($z_i = 3$), in fact:

$$\begin{array}{|c|c|c|c|} \hline & 0 & 0 & \\ \hline 0 & 3 & 3 & 0 \\ \hline & 0 & 0 & \\ \hline \end{array} \longrightarrow \begin{array}{|c|c|c|c|} \hline & 1 & 0 & \\ \hline 1 & -1 & 4 & 0 \\ \hline & 1 & 0 & \\ \hline \end{array} \longrightarrow \begin{array}{|c|c|c|c|} \hline & 1 & 1 & \\ \hline 1 & 0 & 0 & 1 \\ \hline & 1 & 1 & \\ \hline \end{array} \quad (3.18)$$

and in the case $z_i \geq 4$ or $z_j \geq 4$ or both, the same result would have been obtained, any possible rule we choose to use, as proved in 2. This fact can be better understood recalling the relations (2.6) satisfied by the operators a_i and a_j , with i and j corresponding to the ones in (3.16):

$$a_i^4 = a_{i_1} a_{i_2} a_{i_3} a_j \quad (3.19a)$$

$$a_j^4 = a_{j_1} a_{j_2} a_{j_3} a_i \quad (3.19b)$$

If we restrict the attention on recurrent configurations where inverses of a_i exist it is possible to multiply side by side the two equalities obtaining:

$$a_i^4 a_j^4 = a_{i_1} a_{i_2} a_{i_3} a_j a_{j_1} a_{j_2} a_{j_3} a_i \quad (3.20)$$

and dividing (in group sense) each side by a_i and a_j we have the following equality:

$$a_i^3 a_j^3 = a_{i_1} a_{i_2} a_{i_3} a_{j_1} a_{j_2} a_{j_3} \quad (3.21)$$

that is the same of (3.19) for the cluster toppling rule, furthermore this rule generalizes for arbitrary subsets of V . This permit us to state that the different toppling rules we have introduced bring to the same group presentation (and then to the same group structure) for the abelian group associated to the recurrent configurations of the ASM.

We recall now that for the model with the standard toppling rule we have an easy characterization for the subsets F of the graph that are forbidden subconfiguration (FSC), that is:

$$\text{if } \forall i \in F \quad z_i < \sum_{\substack{j \neq i \\ j \in F}} (-\Delta_{ij}) \quad \implies \quad F \text{ is a FSC} \quad (3.22)$$

As obvious with the new rules just introduced, some forbidden subconfigurations of the standard ASM can become reachable by adding sand and toppling, e.g. the simplest forbidden configuration in the case of standard toppling rules, $\begin{bmatrix} 0 & 0 \end{bmatrix}$, is easily reachable if we allow the 2-cluster toppling rule, in fact it can simply turn up as result of the basic 2-cluster toppling $\begin{bmatrix} 3 & 3 \end{bmatrix} \rightarrow \begin{bmatrix} 0 & 0 \end{bmatrix}$. It is also possible to characterize the forbidden subconfigurations with respect to a given I -toppling rule, we have:

$$\text{if } \forall I \subseteq F \quad \sum_{j=1}^k z_{i_j} < \sum_{\substack{j \in F \setminus I \\ \ell \in I}} (-\Delta_{\ell j}) \quad \implies \quad F \text{ is a FSC} \quad (3.23)$$

this yielding to the possibility that a transient configuration with respect to a \mathcal{L}' toppling rule becomes recurrent for a \mathcal{L}'' toppling rule, with $\mathcal{L}'' \supset \mathcal{L}'$.

Furthermore some configurations stable with respect to a \mathcal{L}' toppling rule become unstable if we allow \mathcal{L}' to increase up to \mathcal{L}'' , e.g. the basic unstable configuration $\begin{bmatrix} 3 & 3 \end{bmatrix}$ for the dimer-toppling rule is perfectly stable in the framework of toppling only for $z_i \geq \bar{z}_i$. Moreover the fact that the group structure of the associated group remains unchanged under the addition of the new toppling rules, yields the number of group elements $g \in \mathcal{G}$ to be the same in the two cases, this forces the number of recurrent configurations to be the same, as the order of group associated, i.e. as many stable recurrent becomes unstable, as transient become recurrent, for each enlargement of \mathcal{L} .

In this framework, we see how, remaining unchanged the number of recurrent configurations and growing up the number of unstable configurations, since the set of \mathcal{L} -stable configurations becomes a subset of the original set of stable configurations $S = \{0, 1, 2, 3\}^{|V|}$, in some sense the transient configurations that become allowed must correspond to some newly unstable configurations. This kind of symmetry between the two sets, yields to suppose the existence of a bijection between

unstable configurations for \mathcal{L}'' toppling rules and transient configurations for \mathcal{L}' toppling rules, with $\mathcal{L}'' \supset \mathcal{L}'$. This procedure of enlarging the set of unstable configuration, and at the same time to shrink the set of transient configuration yields to the possibility to completely suppress the set of the transient configurations and to have that the recurrent configurations become all the stable configurations. This situation is reached by letting

$$\mathcal{L} = \{\text{all the subsets of } V\} \quad (3.24)$$

An interesting example is the lattice 3×1 in which the number of configurations is not huge and we can directly check this statement.

$\mathcal{L} = \mathcal{L}_{std}$	$\mathcal{L} = \mathcal{L}_{std} \cup \{i_1, i_2\}$	$\mathcal{L} = \mathcal{L}_{std} \cup \mathcal{L}_{max}$	
<table border="1" style="border-collapse: collapse; width: 60px; height: 20px; margin: 2px;">0</table> <table border="1" style="border-collapse: collapse; width: 60px; height: 20px; margin: 2px;">0</table> <table border="1" style="border-collapse: collapse; width: 60px; height: 20px; margin: 2px;">0</table>	<table border="1" style="border-collapse: collapse; width: 60px; height: 20px; margin: 2px;">0</table> <table border="1" style="border-collapse: collapse; width: 60px; height: 20px; margin: 2px;">1</table> <table border="1" style="border-collapse: collapse; width: 60px; height: 20px; margin: 2px;">0</table>	<table border="1" style="border-collapse: collapse; width: 60px; height: 20px; margin: 2px;">0</table> <table border="1" style="border-collapse: collapse; width: 60px; height: 20px; margin: 2px;">0</table> <table border="1" style="border-collapse: collapse; width: 60px; height: 20px; margin: 2px;">0</table>	<table border="1" style="border-collapse: collapse; width: 60px; height: 20px; margin: 2px;">3</table> <table border="1" style="border-collapse: collapse; width: 60px; height: 20px; margin: 2px;">3</table> <table border="1" style="border-collapse: collapse; width: 60px; height: 20px; margin: 2px;">3</table>
<table border="1" style="border-collapse: collapse; width: 60px; height: 20px; margin: 2px;">0</table> <table border="1" style="border-collapse: collapse; width: 60px; height: 20px; margin: 2px;">0</table> <table border="1" style="border-collapse: collapse; width: 60px; height: 20px; margin: 2px;">$\frac{1,2}{3}$</table>	<table border="1" style="border-collapse: collapse; width: 60px; height: 20px; margin: 2px;">0</table> <table border="1" style="border-collapse: collapse; width: 60px; height: 20px; margin: 2px;">0</table> <table border="1" style="border-collapse: collapse; width: 60px; height: 20px; margin: 2px;">$\frac{1,2}{3}$</table>	<table border="1" style="border-collapse: collapse; width: 60px; height: 20px; margin: 2px;">0</table> <table border="1" style="border-collapse: collapse; width: 60px; height: 20px; margin: 2px;">0</table> <table border="1" style="border-collapse: collapse; width: 60px; height: 20px; margin: 2px;">$\frac{1,2}{3}$</table>	<table border="1" style="border-collapse: collapse; width: 60px; height: 20px; margin: 2px;">3</table> <table border="1" style="border-collapse: collapse; width: 60px; height: 20px; margin: 2px;">3</table> <table border="1" style="border-collapse: collapse; width: 60px; height: 20px; margin: 2px;">$\frac{0,1}{2}$</table>
<table border="1" style="border-collapse: collapse; width: 60px; height: 20px; margin: 2px;">$\frac{1,2}{3}$</table> <table border="1" style="border-collapse: collapse; width: 60px; height: 20px; margin: 2px;">0</table> <table border="1" style="border-collapse: collapse; width: 60px; height: 20px; margin: 2px;">0</table>	<table border="1" style="border-collapse: collapse; width: 60px; height: 20px; margin: 2px;">3</table> <table border="1" style="border-collapse: collapse; width: 60px; height: 20px; margin: 2px;">3</table> <table border="1" style="border-collapse: collapse; width: 60px; height: 20px; margin: 2px;">$\frac{0,1}{2,3}$</table>	<table border="1" style="border-collapse: collapse; width: 60px; height: 20px; margin: 2px;">$\frac{1,2}{3}$</table> <table border="1" style="border-collapse: collapse; width: 60px; height: 20px; margin: 2px;">0</table> <table border="1" style="border-collapse: collapse; width: 60px; height: 20px; margin: 2px;">0</table>	<table border="1" style="border-collapse: collapse; width: 60px; height: 20px; margin: 2px;">$\frac{0,1}{2}$</table> <table border="1" style="border-collapse: collapse; width: 60px; height: 20px; margin: 2px;">3</table> <table border="1" style="border-collapse: collapse; width: 60px; height: 20px; margin: 2px;">3</table>
<table border="1" style="border-collapse: collapse; width: 60px; height: 20px; margin: 2px;">0</table> <table border="1" style="border-collapse: collapse; width: 60px; height: 20px; margin: 2px;">1</table> <table border="1" style="border-collapse: collapse; width: 60px; height: 20px; margin: 2px;">0</table>	<table border="1" style="border-collapse: collapse; width: 60px; height: 20px; margin: 2px;">3</table> <table border="1" style="border-collapse: collapse; width: 60px; height: 20px; margin: 2px;">3</table> <table border="1" style="border-collapse: collapse; width: 60px; height: 20px; margin: 2px;">$\frac{0,1}{2,3}$</table>	<table border="1" style="border-collapse: collapse; width: 60px; height: 20px; margin: 2px;">0</table> <table border="1" style="border-collapse: collapse; width: 60px; height: 20px; margin: 2px;">1</table> <table border="1" style="border-collapse: collapse; width: 60px; height: 20px; margin: 2px;">0</table>	<table border="1" style="border-collapse: collapse; width: 60px; height: 20px; margin: 2px;">3</table> <table border="1" style="border-collapse: collapse; width: 60px; height: 20px; margin: 2px;">2</table> <table border="1" style="border-collapse: collapse; width: 60px; height: 20px; margin: 2px;">3</table>
8 transients	4 recurrents 4 unstables	8 recurrents	8 unstables

3.2 The operator $N_i = a_i^\dagger a_i$

Until this point we worked with the abelian operators a_i of the group \mathcal{G} associated with the ASM, defined as the ones which add a grain in i and let the configuration relax if necessary. It is possible to complementary define the operators a_i^{-1} inverses of a_i and to find their explicit action as shown in [9]. In order to obtain it, must be used the already introduced concept of forbidden subconfigurations (2.16) and the new elementary operation of *untoppling*.

We define the *untoppling rule* the rule through which if, at site i , the height becomes for some reason negative, it is increased by Δ_{ii} and the heights in the other sites j are decreased by $-\Delta_{ij}$, where Δ is the usual toppling matrix of the sandpile. Shortly we can write

$$\text{if } z_i < 0 \implies z_j \rightarrow z_j + \Delta_{ij} \quad \forall j \quad (3.25)$$

If eventually after this updating the height at some other site becomes negative, then we let them untopple following the (3.25). This rule is exactly the symmetric counter-part of the toppling rule (3.2) for the model in which all the heights are trasformed as follows

$$z_i \rightarrow 4 - z_i \quad (3.26)$$

Thus we don't have to worry about the order we choose to perform the different untopplings, indeed they satisfy an abelian property exactly as the standard toppling rule does.

Instead of defining a_i^{-1} we define a new, but similar, operator a_i^\dagger from the space of stable configurations to itself. It effectively acts as follows: given a stable configuration $C = \{z_j\}$, the configuration $a_i^\dagger C = \{z'_j\}$ is the one in which $z'_i = z_i - 1$, and, in the case $z'_i < 0$ after the decreasing, the necessary untoppling are performed in order to obtain an allowed configuration. This is not the same as a_i^{-1} , indeed in that case, after the action of a_i^\dagger , we have to make a burning test to check if the configuration is or not recurrent, and in the case it is transient, a sort of inverse avalanche of the FSC found with the burning test is performed, this procedure is repeated until the configuration becomes recurrent. This fact suggests the property of the a_i^\dagger 's to bring back, in some cases, the recurrent into transient configurations.

We can now define the operator

$$N_i = a_i^\dagger a_i \quad (3.27)$$

Clearly this operator does not commute with the whole operator algebra of the sandpile, indeed the action of a_i^\dagger can decrease the height in a site where otherwise the action of a_i would have generated an avalanche. Now we study the repeated action of N_i on the maximally filled configuration C_{max} , that is $z_i = 3$ for all i , of a square lattice rectangular-shaped. We choose to act on this particular configuration because the action of N_i on it isn't trivial, at the first step, for every site; indeed there are many possible configurations for which the action of N_i is trivial, and so correspond to doing nothing, for some i . Given N_i , the cases for which $N_i C = C$ are the following:

- (i) if $z_i < 3$, in this case the first added particle does not bring to any toppling and the action of a_i^\dagger simply restore the initial height;
- (ii) if $z_i = 3$ and no one of its nearest-neighbors, j , has maximal height ($z_j = 3$), indeed in this case the action of a_i lead up to a toppling, just one, letting $z_i = 0$; the following action of a_i^\dagger involves one untoppling and restore the initial situation.

N_i acting on configuration C_{max} creates diagrams that pictorially seems "scattering diagrams". We tested this fact by the help of a computer program written by Creutz [19], this program represents each different height value with a different colour:

$$\blacksquare z_i = 3; \quad \color{blue}\blacksquare z_i = 2; \quad \color{red}\blacksquare z_i = 1; \quad \color{gray}\blacksquare z_i = 0$$

thus in the following we will indifferently speak about a site i of height $z_i = 2$ as a "2-height" site or as a "blue" site.

Let us speak about what happens with the action of N_i : we will discuss the fenomenology on a square-shaped lattice. The first hit creates a central square

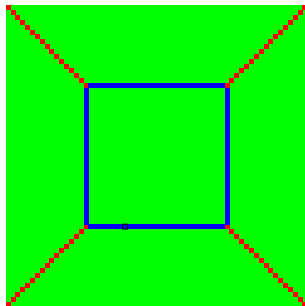


Figure 3.1 configuration after a single hit of N_i in the site marked in black

of blue sites with 4 beams of red sites departing from its vertices and connecting to the corner of the lattice (fig. 3.1). We define this new objects as some defect in the originally homogeneous background of height 3, i.e. $z_i < 3$, that present a periodicity with a certain period (k_x, k_y) , obviously integer, being the ASM settled in a lattice; in the following, with abuse of notation, we will call them *propagators*, and we will indicate the component k_x and k_y of the periodicity as the *momenta* of the propagator. Acting with N_i more time on the just reached configuration, bring to different possible results, neglecting the cases in which the action is trivial. Choosing the i inside the blue square just formed, that we can consider in some way as a loop of blue propagators, the action of N_i simply contracts the initial square into the one tangent to the point i chosen. On the other hand, choosing i in one of the four external trapezoids, it seems that, from the corresponding corners, some “new mass” reaches the diagram, changing the propagators that migrate and become of different shape, and of different momentum. Continuing as just presented it is possible to create many different propagators for as many values of k_x and k_y we want.

3.2.1 The ASM-propagators

Having produced some data about these “ASM-propagators”, and having spanned many possible different shapes of the above defined “propagators”, it is possible to state some apparent rule they follow, although we did not succeed still in proving the more “exotic” of them.

1) It is possible for the propagators to meet in some vertices, in general meeting point for three of them, just as two of them scatter in a new propagator. This happens with a surprising conservation law, indeed considering the momenta of the propagators as a flow, then in a process the following relation holds

$$(p_x, p_y) + (q_x, q_y) = (k_x, k_y) \quad (3.28)$$

the momentum along direction x and y is conserved, so

$$p_x + q_x = k_x \quad \text{and} \quad p_y + q_y = k_y \quad (3.29)$$

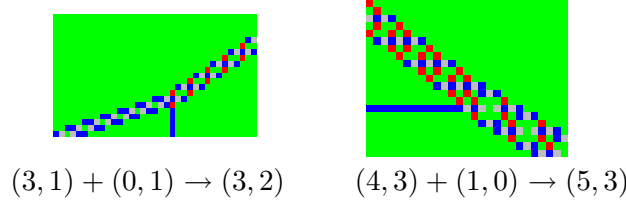


Figure 3.2 example of vertices of scattering

In figure 3.2 are shown some examples

2) When in the diagram a loop forms, composed by the known propagators, then this loop is a forbidden subconfiguration. The action of N_i inside the loop leads up to shrink the loop, until it becomes a single vertex. Otherwise N_i acting in a zone external of any loop (i.e. adjacent to the border), creates a new loop and increase the momenta incident on the corners of the square.

3) A fact true for all the case we studied, is that at each propagator we can associate a quantity defined as the sum of the defects of height with respect to the completely filled configuration in the space of a period (k_x, k_y) . The non-trivial fact is that this quantity, we can call E , satisfies the following relation:

$$E = k_x^2 + k_y^2 \quad (3.30)$$

For example in the case of the propagator $(5, 2)$ we have the following value for E , $E = 25 + 4 = 29$, counting the number of sites with height less than 3 there are 6 of height 0 and 11 of height 2, so the total height defect is $6 \times 3 + 11 = 29 = E$.

4) Propagators (k_x, k_y) with k_x and k_y relatively prime, are named “prime”. These propagators have defined shape, and cannot be composed of other smaller propagators. The propagators in the form (nk_x, nk_y) are generally composed of n propagators (k_x, k_y) that propagate parallelly. The only exception we know is the propagator $(2, 0)$, it has the special property to present two different possible shape, in fact it can be two parallel blue lines, but can also be a single red line, however the E of this propagator has the right value 4 in both the shapes of the propagator, if we use accordingly a period of 2, $k_x = 2$.

5) High momentum propagators are much more unstable than the low-momentum ones. So it is easy to break their structure by acting with N_i on the lattice. Furthermore in scattering events of high momentum propagators the structure of the vertex is not easy to understand, but it is possible to recognize some fine structures composed of low momentum operators.

6) In the case a propagator (k_x, k_y) can be written as $(p_x + q_x, p_y + q_y)$ with p_x, p_y near to q_x, q_y , it seems to behave like two propagators $(p_x, p_y), (q_x, q_y)$ that propagate parallelly and exchange a particle every half period. In particular this feature is clear for family of propagators close to the two families $(k, k - 1)$ and $(k, 1)$, e.g. $(9, 2)$ and $(9, 7)$ as can be seen in figura 3.6.

7) In the case the initially maximally filled configuration has some defects (e.g. a single point of height 0, 1 or 2) on condition that this defects does not produce a forbidden subconfiguration, the dynamics induced by the N_i 's on C_{max} is not perturbed by their presence. It happens that the propagators seen acting on C_{max} as initial configuration are exactly the same in the regions where the defects are not present, in regions where is localized a defect, the propagators, seen as height defects, simply decrease the height of the defect present in the initial configuration, in the case the height becomes negative, an untopping operator acts in order to have an allowed configuration. When the propagators move over, then the initial configuration is perfectly restored, so the dynamics is not affected by any perturbation.

8) When there is a loop of propagators, as said above the action of N_i in its inner part, shrink it, the non-trivial fact is that every possible sequence of operators that completely shrinks the loop to a “tree” diagram connecting the propagators incoming in the loop, brings to the same result, irrespectively of the number of operators we used or the positions where they act, on condition that they all act inside the loop (i.e. if the loop is embedded into a box with no other loops, all N_i act on components of height 3 not connected to the border).

Furthermore we have found some typical patterns for particular families of propagators. We present the rule to build the propagator for the families $(k, 1)$ and $(k, k - 1)$ for k greater than 1. The pattern for generic $(k, 1)$, (fig. 3.3), is formed by a sequence of blue squares $(k - 1) \times (k - 1)$ with diagonal composed of grey sites, each one shifted of one site from the previous and linking to it by a column of $k - 2$ green sites and 1 more blue site for side.

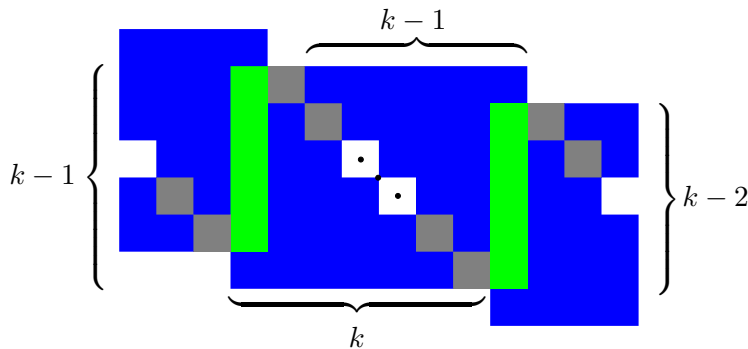


Figure 3.3 characterization of $(k, 1)$ generic propagator

The pattern for generic $(k, k - 1)$, (fig. 3.4), is in some sense similar, up to a rotation of 45° , to the one for the $(k, 1)$ family. Indeed it presents a sequence of rombi with each half, divided by the diagonal (horizontal w.r.t. the lattice directions), composed of a triangle, of sites red and green, arranged in echelon formation, whose height is $k - 2$; then the diagonal is long $2k - 1$ sites, k of them being blue and $k - 1$ grey. These structures are linked such that the tip of the triangle is connected to the end of the diagonal of the previous rombus.

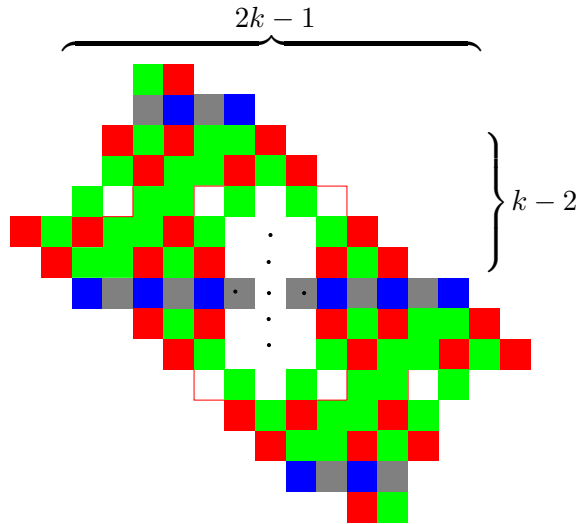


Figure 3.4 characterization of $(k, k - 1)$ generic propagator

Some examples of components of these families for particular value of k are presented in figure 3.5

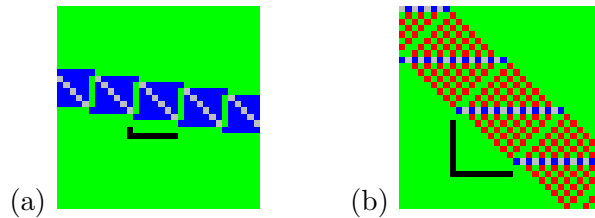


Figure 3.5 examples of propagators: (a) $(7, 1)$ belonging to the family $(k, 1)$; (b) $(9, 8)$ belonging to the family $(k, k - 1)$

These two families have also an easy characterization for the basic scattering vertices of the processes

$$(k, 1) + (1, 0) \rightarrow (k + 1, 0) \quad \text{and} \quad (k, k - 1) + (1, 1) \rightarrow (k + 1, k) \quad (3.31)$$

The first scattering is obtained simply enlarging the square of the composing the $(k, 1)$ propagator. When the single blue line of the $(1, 0)$ propagator meets the wider propagator, it adds to the square in the side parallel to its direction, enlarges the square and the the structure repeats with the expected periodicity. As for the general structure of the propagator the similitude between the $(k, 1)$ and $(k, k - 1)$ propagators is preserved for the pattern of elementary scattering, indeed the red line at 45° representing the $(1, 1)$ propagator, when meets the $(k, k + 1)$ adds to the

triangle composing the rombhus, enlarging it, and the enlarged rombhus repeats with the expected periodicity.

In the prescription on how to shrink a loop, it is hard to distinguish in some “intrinsic” way which green regions are “inside” a propagator (e.g. as in figure 3.5 for prop. $(k, 1)$ and $(k, k - 1)$) and which are inside a subloop which is almost shrinked out. If one impose to squeeze all the green regions not connected to the border, one obtain a new family of propagators, corresponding to the reduction of the previous one w.r.t. the prescription above. As for the *natural* propagators this new ones has similar scattering rules and satisfy the periodicity property we used to define the natural propagators. In figures 3.6 and 3.7 we report the tabular of natural and squeezed propagators.

To obtain the figures presented in this section we have been helped by the program `xsand` written by M. Creutz, besides other programs we wrote in order to study the high-order propagators [19]

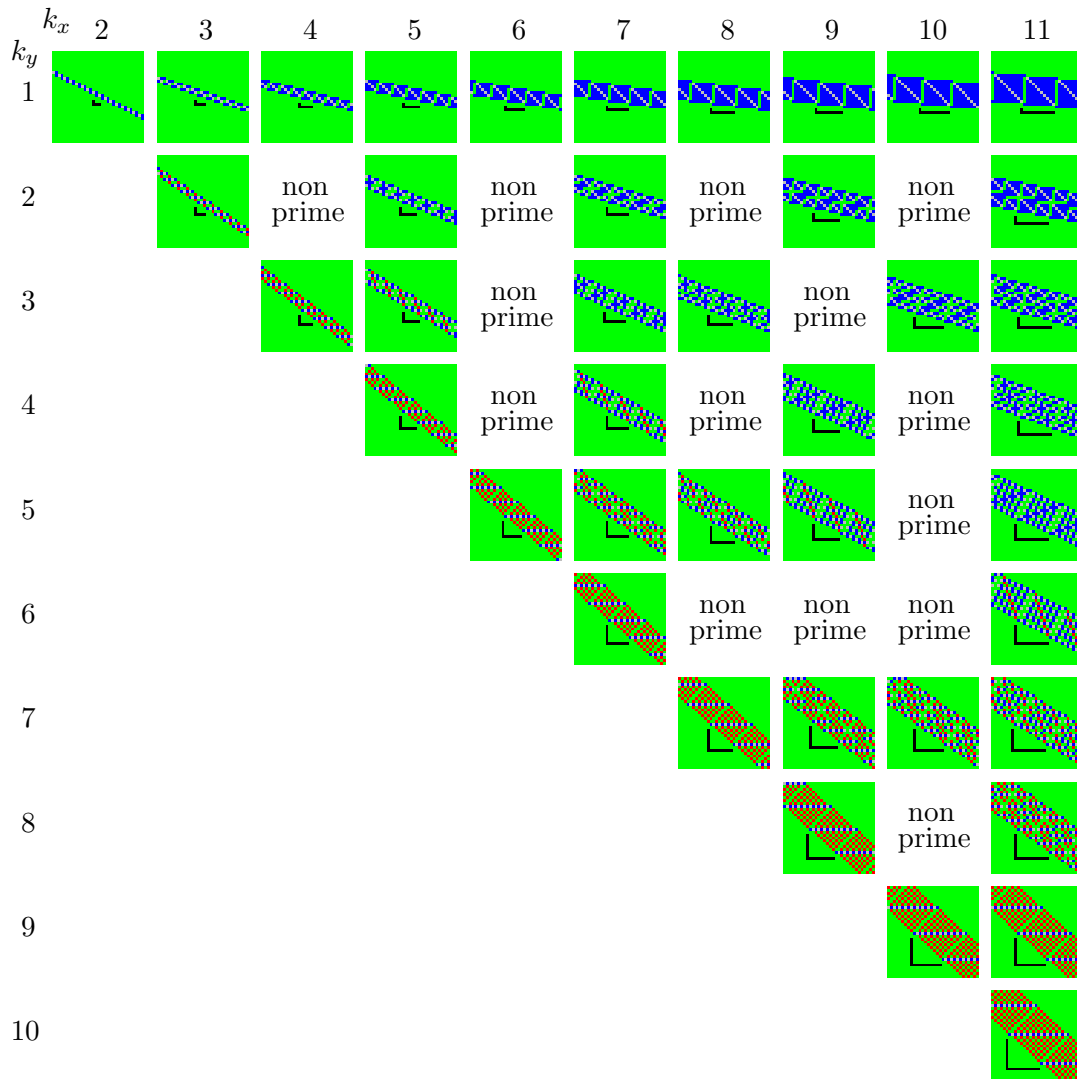


Figure 3.6 natural propagators

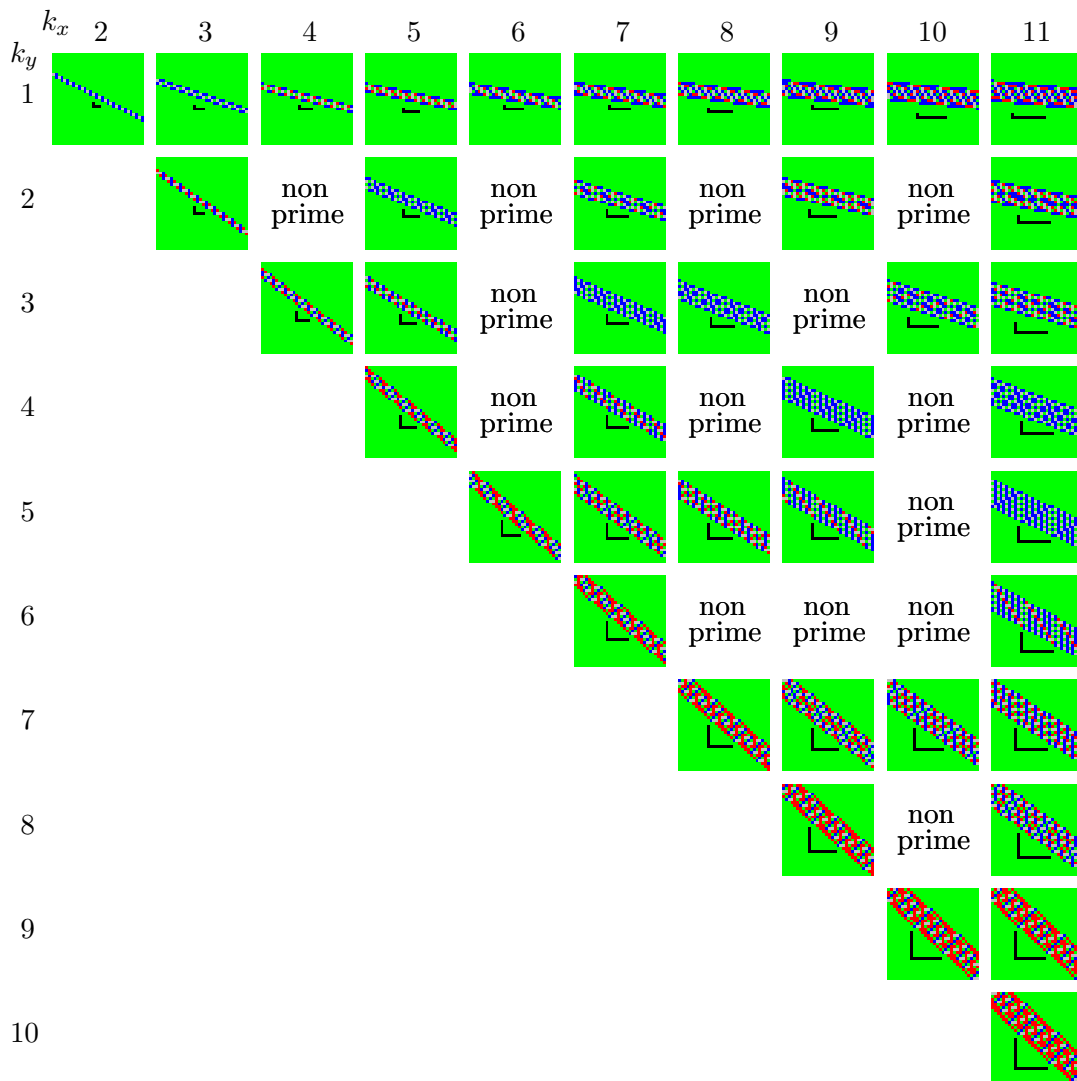


Figure 3.7 squeezed propagators

3.3 Stationary state

In this last section of the chapter we study the possibility to act on the configuration C_{max} of a given lattice with the operator N_i uniformly on the lattice, as many time as it is possible until no more site gives rise to a non-trivial action of N_i . A priori there is no guarantee for this process to stop in a finite time nor to reach the same state following a different sequence of operators $N_{i_k} N_{i_{k-1}} \cdots N_{i_1}$ (e.g. having a different number of operators, or taking the same set of operators in different order), but surprisingly this fact happens, and in the following we will give the reason for this fact. We call *stationary state* the configuration reached at the end of this process.

This uniqueness of the stationary state can be explained by the fact that the action of N_i is in fact just a tool to perform the 2-cluster toppling rule only in the clusters to which the site i belong, and only if this cluster were unstable in the sense of (3.15), indeed the cases (i) and (ii) in which the action of N_i is trivial are exactly when i does not belong to any unstable 2-cluster. In this perspective the action repeated with N_i until no more sites permit an untrivial action of the operator, simply corresponds to reach the stable configuration with respect of the 2-cluster toppling rule defined above. Furthermore the theorem 3 states that the order with which we choose to perform the different topplings, that is the order with which we choose to act with the different N_i , is irrelevant for the final result. Indeed the final stable configuration is unique, and each different “history” must give the same result.

Other interesting facts about this particular configuration are the following:

1) The patterns obtained are shape depending, but they seems to follow the same guidelines, in particular for rombhus and square we found a bulk part composed of a grid

2	3
1	2

, otherwise the part near the boundary seems to exhibit particular patterns that have some influence due to the corners of the chosen shapes. We also studied the patterns in a circular shape, in order to minimize the effects of the corners, in this case the pattern found only in the bulk for the square and the rombhus fills entirely the circle, apart a boundary zone, thin with respect to the diameter of the circle, see figure 3.8.

2) The dynamics converging to the stationary state has an interesting property, in particular in the case of the circle, after a initial state of “bubbles” mainly of propagators (0,1) and (1,1), the system reaches a moment in which only the internal part needs to change further on, the part mantains the circular shape of the whole lattice, and then collapse in the final stationary state , see figure 3.9.

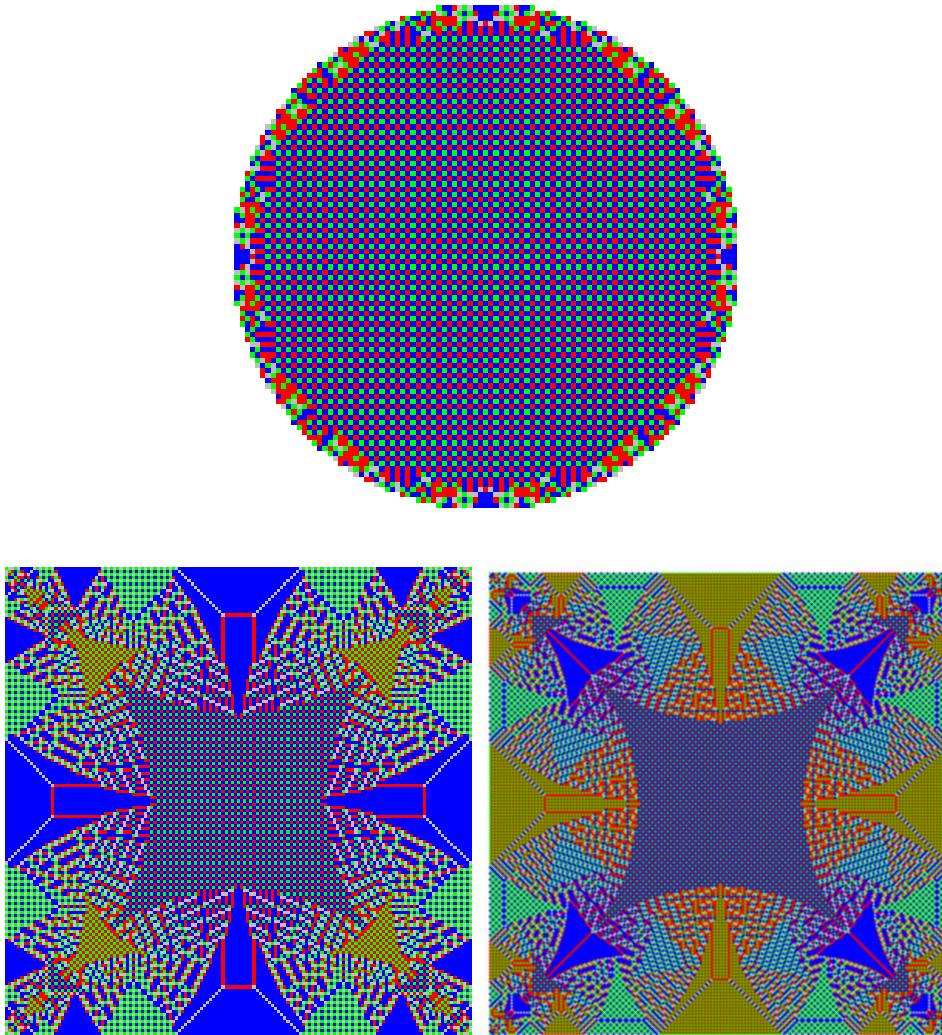


Figure 3.8 Example of stationary state for a square of side $L = 151$, a rhombus with diagonal $d = 299$ and a circle with diameter $D = 97$

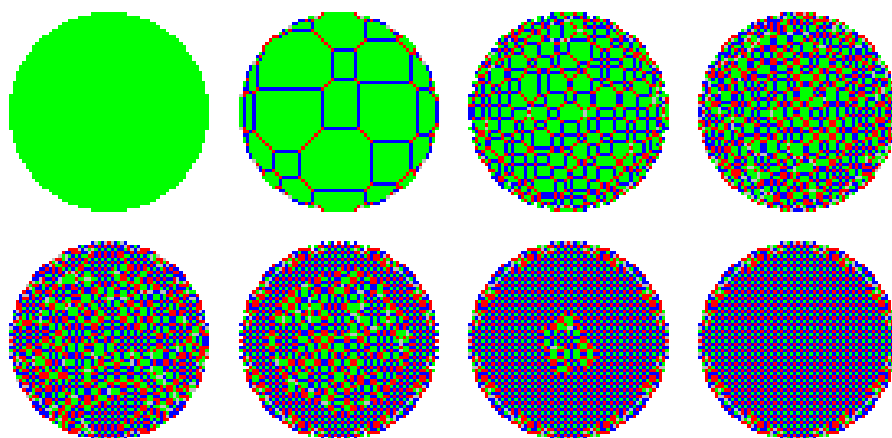


Figure 3.9 Evolution of the state of a circle of diameter 61

4. An algorithm for uniform sampling of trees

In chapter 2 we reported how to construct an explicit basis for the space of recurrent configurations \mathbf{R} . We want now to show how it is possible to use this basis to obtain an algorithm with polynomial-time worst-case complexity for exact sampling of the recurrent configurations and, through the bijection obtained *via* burning test of the ASM, of trees of the graph associated.

When studying the ASM on an N sites square lattice, as presented in section 2.5.2, we found that the relations (2.44) give a presentation of the group \mathcal{G} associated to the ASM, in terms of the $g \times g$ integer matrix $n_{yy'}$ where g is the rank of the group. The elements of $n_{yy'}$ are obtained solving the linear recursive relation (2.40). Thus in this case is not necessary, in order to examine the group structure of \mathcal{G} , to work with the huge $N \times N$ toppling matrix Δ , indeed the structure of \mathcal{G} can be determined by the normal form decomposition of $n_{yy'}$.

This allow us to determine explicitly the form of the generators \hat{e}_i and their period. We recall that it is possible, in the case of a rectangular-shaped square lattice $L_1 \times L_2$, to find an overcomplete set of generators with periods d_i , but in any case the d_i found through the Smith normal form satisfy the relations $d_1 \geq d_2 \geq \dots d_g > 1$ with d_i an integer multiple of d_{i+1} . In the case of a square-shaped lattice the number L of generators is minimal, and this allows to compute the generators. To characterize the algorithm, we need a bound for the value of periods d_i . In order to obtain a bound for the value of the various periods of \hat{e}_i , first we recall the following relation

$$\prod_{i=1}^g d_i = |\mathcal{G}| \quad (4.1)$$

here g is the number of a minimum set of generators. Now we note that the number of allowed configuration is 4^{L^2} , and it is much greater than the number of recurrent configuration, that we know to be $\det \Delta$, furthermore the number of recurrent configuration is equal to the order of \mathcal{G} as stated in (2.9). This relations, together with the (4.1) yields to write:

$$d_i < |\mathcal{G}| = \det \Delta < e^{aL^2} \quad (4.2)$$

with $a = \log 4$. So an upper bound for d_i is e^{aL^2} , but it still desirable to obtain a more restrictive bound.

It is possible to compute for each generator \hat{e}_i its 2^k -powers, indeed in the following procedure they will be useful tools for computing some particular configurations. This task is done by subsequent doubling of the configuration associated to the generator, that is

$$(\hat{e}_i)^{2^k} = (\hat{e}_i)^{2^{k-1}} \oplus (\hat{e}_i)^{2^{k-1}} \quad (4.3)$$

Furthermore, each sum of stable configurations takes a polynomial time, at most of order L^4 , to be performed¹. This lets evaluate the time needed to obtain the sequence of the 2^k -powers for a given \hat{e}_i , that is $t \sim kL^4$ where k is the number of 2^k -powers needed, dependent on the period d_i , chosen as

$$k = \lfloor \log_2(d_i) \rfloor \quad (4.4)$$

As said before the period grows as e^{aL^2} so k is order $L^2 \times$ some suitable constant. At this point it is possible to write the estimated time to obtain all the 2^k -power-configurations of the various generators

$$t \sim L^2 L^4 L = L^7 \quad (4.5)$$

where the factor L^2 comes from the number of 2^k -powers needed for each generator, L from the number of generators and L^4 from the time needed to perform each sum of configurations, with sitewise addition plus relaxation.

Furthermore the space in memory needed to store the configurations, in order to use them in the following part of the algorithm, is

$$\text{memory} \sim L^2 L^2 L \quad (4.6)$$

where L comes from the number of generators, and a first L^2 for the number of 2^k -powers, a further L^2 from the space needed for each configuration to be stored, being a configuration of an $L \times L$ lattice.

It is now easy to obtain the exact sampling for the recurrent configurations of the sandpile. Indeed, forming the generators a basis of the set \mathbf{R} , at each given recurrent configuration C can be associated a vector $\vec{n}(C)$ that represent it in terms of the basis, that is

$$C = \left(\sum_i n_i(C) \hat{e}_i \right) \oplus C_{id}. \quad (4.7)$$

This reduce the sampling of the recurrent configuration to the sampling of a vector \vec{n} such that each of its components is $0 \leq n_i < d_i$. Then using the relation (4.7) we

¹Define $I(\{z_i\}) = \sum_i z_i r^2(i)$, where $r(i)$ is the distance of i from the center of the square. When a toppling occurs on the border, say that the particle leaving the system remains on the lattice site immediately out of the square. With this rule, each toppling increases I by 4, and the total mass (including the particles out of the border) remains fixed. The worst case is that all particles go out at the corners (where $r^2(i) \sim L^2/2$), so that $I_{final} - I_{begin} \gtrsim \sum_i z_i (L^2/2 - r^2(i))$. As at each site $z_i \leq 6$ (during the parallel toppling), this quantity is further bounded by $\sim 6L^4 \int_{-1/2}^{1/2} dx \int_{-1/2}^{1/2} dy (\frac{1}{2} - x^2 - y^2) = 2L^4$, so the number of toppling is $\lesssim L^4/2$.

obtain the configuration desired. The last step for obtain the sampled recurrent configuration is, in fact, a simple sum of generator's configurations. This sum is in principle simple, but in practice there is a computational problem. Indeed there is a huge number of configuration to be summed, that comes from the fact that in average each period d_i grows exponentially as said in the beginning of the chapter. To solve this problem we transform the integers n_i sampled in their binary form $n_i = 010\dots 011101$ and then, instead of perform the relaxation of $n_i\hat{e}_i$, we write

$$n_i = \sum_{j=0}^{\sim L^2} b_{ij}2^j \quad b_{ij} \in \{0,1\} \quad (4.8)$$

and we take

$$\bigoplus_{i=1}^L \bigoplus_{b_{ij}=1} (2^j \hat{e}_i) \quad (4.9)$$

which are at most L^3 stable configurations, so that summing them even in a naive way takes a time $\sim L^4 L^3 = L^7$.

So we prove a rigorous bound for the exact sampling of spanning trees on $L \times L$ square geometry of L^7 -time and L^5 -space for the preprocessing, and L^7 -time and L^2 -space (but quite generously estimated) for each independent sampling.

In a cylindrical geometry, with the y -sides taken periodic, one of the two x -side open and the other closed, particular symmetry properties permits to further on speed up the algorithm. Indeed the space needed to store the 2^k -powers of generators is decreased of a factor L due to the periodicity, and the time required to create all the configurations $2^k \hat{e}_i$ also decrease by a factor L , as $2^k \hat{e}_i$ and $2^k \hat{e}_j$ only differ by a translation on the cylinder, so the preprocessing is time $\sim L^6$ space $\sim L^4$ in this case.

5. Monte-Carlo algorithms for the Potts model

One of the most important tool for the study of statistical mechanics is the possibility to perform simulations of its models in order to obtain detailed informations about them otherwise unreachable analytically. This is done using a class of computational algorithms that uses stochastic approach to the problem, these algorithms are named *Monte Carlo algorithms*. In particular the Potts model has been widely studied with this method and many different algorithms have been proposed for sampling configurations of the model in different ranges of value of its parameters q and J . In this chapter we give a brief review on some known methods for Monte Carlo simulation, trying to point out the possible problems that each algorithm presents at the various regimes.

5.1 Swendsen-Wang algorithm

One of the most important algorithms for simulating the Potts model was proposed in 1987 by Swendsen and Wang and is known as the Swendsen-Wang cluster algorithm [12]. It simulate the q -state ferromagnetic Potts model at positive integer $q > 1$. The Swendsen-Wang algorithm is based on passing back and forth between the Potts spin representation and the Fortuin-Kasteleyn bond representation (see section 1.3.2), that for a Potts model on a graph $G = (E, V)$ is

$$Z = \sum_{A \subseteq E} q^{C(A)} v^{|A|}. \quad (5.1)$$

Let show explicitly how the algorithm works. Beginning with an arbitrary configuration of Potts spins, we create bonds with probability $p = 1 - e^{-J}$, where J is the coupling constant of the Potts model, between nearest-neighbor sites with the same spin value. No bonds are present between sites containing different spins. If the original spins are now erased, we are left with a configuration of bonds, and clusters, with weights given by (5.1). Note that some of the original clusters of Potts spins may be split into smaller clusters, since bonds do not occur between all sites with the same spin.

The next step is to assign a random Potts value $\sigma \in \{1, \dots, q\}$ to each cluster and the same spin value to each site in the cluster. Then by erasing the bonds

we are now left with a new Potts configuration. The new Potts configuration can differ substantially from the original one, since large portions of large clusters can change colour in a single step.

To see directly that the detailed balance is satisfied, note that every transition between two Potts configurations must pass through some bond configuration. The probability to pass through a bond configuration has a factor p for every bond and a factor q for every cluster regardless of which Potts configuration we started with. However the probabilities differ of a factor $1 - p$ for each missing bond between neighboring sites with the same spin value. Since the probability is uniform for going from a bond configuration to any Potts configuration consistent with it, the ratio of the transition rates is just the exponential of the difference in the Hamiltonian of the two Potts configurations. Since detailed balance is satisfied explicitly for every bond configuration the system can pass through during the transition between two Potts configurations, detailed balance is satisfied for the total transition probability.

This algorithm does not eliminate critical slowing-down, that is a problem connected to the simulations approaching the critical point of the model, but it radically reduces it compared to local algorithms. Much effort has therefore been devoted, for both theoretical and practical reasons, to understanding the dynamic critical behavior of the Swendsen-Wang algorithm as a function of the spatial dimension d and the number q of Potts spin states. Anyway this algorithm has the limitation to allow the simulation only for positive integer value of q .

5.2 Chayes-Machta algorithm

A further advance was made in 1998 by Chayes and Machta [24], who devised a cluster algorithm for simulating the random-cluster model (see section 1.3.2) — which provides a natural extension of the Potts model to non-integer q — at any real $q > 1$. The Chayes-Machta algorithm generalizes the Swendsen-Wang algorithm and in fact reduces to it when q is an integer.

We consider the *Fortuin-Kasteleyn random-cluster model* with parameter $q > 0$ defined on any finite graph $G = (V, E)$ by the partition function

$$Z = \sum_{A \subseteq E} q^{k(A)} \prod_{e \in A} v_e \quad (5.2)$$

where A is the set of occupied bonds, $k(A)$ is the number of connected components in the graph (V, A) and $\{v_e\}$ are nonnegative edge weights.

At our aim, it is convenient to consider a more general partition function, the *generalized random-cluster model*

$$Z = \sum_{A \subseteq E} \left(\prod_{e \in A} v_e \right) \left(\prod_{i=1}^k W(H_i) \right) \quad (5.3)$$

where H_1, \dots, H_k are the connected components of the graph (V, A) , and $\{W(H)\}$ are non-negative weights associated to the connected subgraphs H of G . The model reduces to the Fortuin-Kasteleyn model if $W(H) = q$ for all H ; other special cases include the Fortuin-Kasteleyn representation for the Potts model in a magnetic field and various loop models.

Now let m be a positive integer, and let us decompose each weight $W(H)$ into m non-negative pieces, any way we like

$$W(H) = \sum_{\alpha=1}^m W_{\alpha}(H) \quad (5.4)$$

The first step of the generalized Chayes-Machta algorithm, given a bond configuration A , is to choose, independently for each connected component H_i , a “color” $\alpha \in \{1, \dots, m\}$ with probabilities $W_{\alpha}(H_i)/W(H_i)$; this color is then assigned to all the vertices of H_i . The vertex set V is thus partitioned into

$$V = \bigcup_{\alpha=1}^m V_{\alpha}. \quad (5.5)$$

It is not hard to see that the bond configuration is nothing else than a generalized random-cluster model with weights $\{W_{\alpha}(H)\}$ on the induced subgraph $G[V_{\alpha}]$, independently for each α .

We now can update these generalized random-cluster models on these sublattices by any valid Monte Carlo algorithm. One valid update is “do nothing”; this corresponds to the “inactive” colors of Chayes and Machta. Of course, we must also include at least one non trivial update. The basic idea is to have at least one color for which the weights $W_{\alpha}(H)$ are “easy” to simulate. In particular, when $W(H) = q$ for all H (the standard Fortuin-Kasteleyn random-cluster model), we can take $W_{\alpha}(H) = 1$ for one or more colors α (the so-called “active” colors); the corresponding model on $G[V_{\alpha}]$ is the independent bond percolation, which can be trivially exactly resampled. Since we must have $W_{\alpha}(H) \leq W(H)$, this works whenever $q \geq 1$. More generally if $q \geq k$ we can have k active colors and a fraction $\sim \frac{k}{q}$ of edges is exactly resampled (within the given partition) at each step. If q is an integer and we take $k = q$, we recover the standard SW algorithm.

This algorithm has the fundamental improvement, respect to the Swendsen-Wang algorithm, to permit the simulation also for non integer values of q , thus having access to ranges of q corresponding to the general random-cluster model. Although this improvement, it maintains the restriction that does not allow to simulate the model for $q < 1$, range of values interesting in order to study the system for q approaching to zero.

5.3 Sweeny algorithm

One of the simplest possible dynamics for simulating the random-cluster model for a given graph $G = (E, V)$, (5.1), is the local bond-update dynamics first used

by Sweeny [10] in 1983. This algorithm is based on local moves and proceeds as follows:

- (1) we pick a bond $e \in E$ randomly and purpose to change it state (occupied or unoccupied)
- (2) we update the current occupation state of the bond e according to a Metropolis dynamics that is based on the weights given by (5.1), and on the preceding occupation state. In detail, this means that e will become occupied with probability 1 if it connects two different clusters, it will become unoccupied with probability q if it is part of a cluster, indeed its deletion divides a cluster forming two different clusters, and it will remain unoccupied with probability 1 if its addition forms a loop in an already existent cluster.
- (3) return to step 1

This algorithm has the defect to become very slow in $q \ll 1$, indeed the number of accepted moves, at thermal equilibrium, is decreasing linearly with q near zero, this particular problem will be handled in section 6.2.

5.4 Region $q < 1$

The brief review given in the preceedings sections shows how it is possible to simulate the case $q < 1$ only with the Sweeny dynamics, but this dynamics is slow for many different reasons, in fact the local-updating procedure require a big amount of steps before reaching thermalization, or decorrelation from a given configuration. Furthermore in the zone $q \rightarrow 0$ the rate of accepted moves decreases as q . It is our aim to speed up this dynamics to obtain a faster simulation. We will study the possibility to have an algorithm passing back and forth between the random-cluster representation and a representation that enables the unfreezing of observables otherwise blocked.

6. Sampling of Forests

In this chapter we present a Monte Carlo algorithm for the sampling of the random cluster model at low values of q . In this region, and in a particular limit, ($q \rightarrow 0, v/q = t$ fixed), the Fortuin-Kasteleyn representation corresponds to a measure non vanishing only for ensemble of spanning forestsforest, whose number of components approaches to 1 when $T \rightarrow 0$, where T is the weight for each component. We aim to produce the algorithm collecting together a dynamics of Sweeny type (section 5.3), that unfreezes the cluster observables, and a dynamics of ASM type, that mixes the link in each cluster with a uniform probability, as said in chapter 2, and, in particular, can produce big changes when an avalanche occurs after the addition of a particle. As we said above, we want to mix Monte Carlo moves of two different kinds, and also to speed up one of the two dynamics, which otherwise would suffer from (a component of) critical slowing-down due to trivial reasons. These procedures are a bit delicate, and we have to prove that the resulting Markov chain has the proper measure. In order to do this, we discuss a bit these issues in more generality in these three sections 6.1, 6.2 and 6.3.

6.1 Collecting two dynamics together

We consider two different Markov chains with transitions given by moves of type A and B , and with Markov's rate $p_y^{(1)}(x)$ and $p_y^{(2)}(x)$. If they have the same stationary measure $\mu(x)$, this measure is achieved also by the new Markov chain being the union, under some prescriptions of the two preceeding dynamics. Any prescription on which move to use at each temporal step (e.g. deterministic, (A, B, A, B, \dots) , or random with a given probability p , $(A, A, B, A, B, B, B, A, A, \dots)$) is valid with the *caveat* that is given *a priori* and *independent* of the configuration of the system at time t .

We now prove that given these prescriptions, the Markov chain defined by $p_y^{(1+2)}(x)$ has $\mu(x)$ as stationary measure. Indeed, by the general theory of Markov chains, we know that if $\mu(x)$ is a Frobenius vector (eigenvector with eigenvalue 1, all the other λ 's being $|\lambda| < 1$) with respect to the rates

$$\left(p_y^{(1+2)}(x)\right)^k \begin{cases} k = \text{period of the pattern, e.g. } 2 \text{ } (A, B, A, B, \dots) \\ k = 1 \text{ if the pattern is purely random} \end{cases} \quad (6.1)$$

then the Markov chain will converge to the stationary measure $\mu(x)$. Indeed we know that $\mu(x)$ is a Frobenius eigenvector with respect to $p^{(1)}$, being its stationary

measure, and the same holds for $p^{(2)}$ (it is also allowed that unicity of $|\lambda| = 1$ lacks in one of the two moves). Now for linearity we have that $\mu(x)$ is a Frobenius vector also with respect to $ap^{(1)} + (1-a)p^{(2)}$ with $a \in \mathbb{R}$, and this proves the thesis.

We note that the prescription on the choice of which Markov chain use, although independent of the current configuration, can be chosen with respect to the thermodynamic parameters of the system (e.g. its size N or the value of T).

6.2 Boost of slow dynamics

We say that a dynamics is very slow when the probability to make self-moves is much bigger than the probability to reach a different state. When this fact happens for simple structural reasons, and calling the probability to make a self-move – i.e. doing nothing and remain in the same configuration – $p_{self}(x)$, we have that

$$p_{self}(x) = 1 - o(1) \quad (6.2)$$

Evolving the state of the system, it is possible to “boost” it. We suppose also to have

$$p_{self}(x) > p_{self}^{(comp)}(x) \quad (6.3)$$

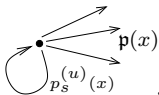
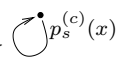
where $p_{self}(x)$ is the probability to make a self-move and $p_{self}^{(comp)}(x)$ is the computable probability of doing nothing. Furthermore we define $p_{self}^{(unk)}(x)$ as:

$$p_{self}^{(unk)}(x) = p_{self}(x) - p_{self}^{(comp)}(x) \quad (6.4)$$

In fact, if the dynamics approaches the desired measure $\mu(x)$ with the rates $\{p_{self}(x), p_y(x)\}$ satisfying the *master equation*, then I can “boost” the dynamics by doing moves with rates

$$\frac{\{p_{self}^{(unk)}(x), p_y(x)\}}{1 - p_{self}^{(comp)}(x)}, \quad (6.5)$$

and then count each configuration in the data histogram *not* with time “1”, but with time “ n ” geometrically distributed with average $\frac{1}{1 - p_{self}^{(comp)}(x)}$. This is just as an ideal process in which with the probability $\mathbf{p}(x) = 1 - p_{self}^{(comp)}(x)$ uses an outgoing

arrow , and with probability $1 - \mathbf{p}(x)$ uses a self-arrow . With this approach $\mathbf{p}(x)$ is just a given parameter depending on x that remains constant during the whole process in which the arrows used are self-arrows .

It is possible to compute the distribution of the expectation values of the time with a single random number $rand()$, using the formula:

$$n = \left\lceil \frac{\ln rand()}{\ln(1 - \mathbf{p}(x))} \right\rceil \quad (6.6)$$

6.3 Boost of collected dynamics

Given an *a priori* dynamics for the combination of two different Markov chains (e.g. A e B presented in section 6.1), this dynamics may become very difficult to simulate when we choose to “boost”, as presented in the previous section, one of the two moves or both of them.

Let suppose to have an “unboosted” dynamics, obtained collecting together the two dynamics with a periodic prescription of period t , e.g. $t = 101$, that can be briefly represented by:

$$A, \underbrace{B, B, \dots, B}_{100}, A, \underbrace{B, B, \dots, B}_{100}, A, B, \dots \quad (6.7)$$

Then the new dynamics can be obtained as sketched in the following diagram:

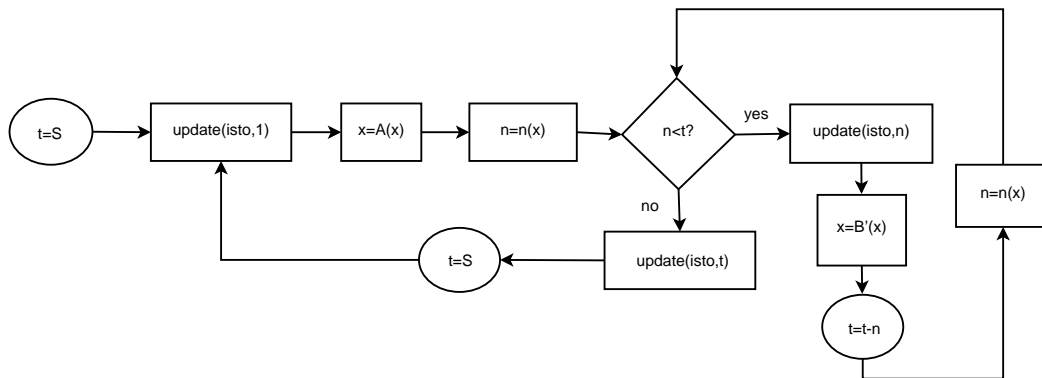


Figure 6.1 flux diagram of the “boosted” union algorithm

where $n(x)$ is the time value computed using the relation (6.6) applied to the current configuration, $update(isto,n)$ means to update the data histogram increasing the counter of time of the value n (i.e. counting each observable in averages with a relative weight n), S is the threshold value which determines the frequency of changing between the two elementary moves we have (for example 100 in (6.7)) and $x = A(x)$ ($x = B'(x) = B_{boost}(x)$) represents the action of the move A (B_{boost} , where B_{boost} is the move boosted as in section 6.2) on the configuration x .

We now report an example of typical code “unboosted” with periodic prescription of period `threshold`:

```

for(t=0;t<t_max;t++)
{
  update(isto,1);
  move A;
  for(c=threshold;c>0;c--)
  {
    update(isto,1);
  }
}

```

```

        move B;
    }
}

```

Here is an example of the same code with a “boosted” dynamics:

```

for(t=0;t<t_max;t++)
{
    update(isto,1);
    move A;
    c=threshold;
    while(c>0)
    {
        n=n(x);
        if(c-n>0)
        {
            update(isto,n);
            c=c-n;
            move B';
        }
        else
        {
            update(isto,c);
            c=0;
        }
    }
}
}

```

6.4 Overview on our algorithm

We present here an algorithm that collects together the Sweeny dynamics displayed in section 5.3 and the ASM dynamics discussed in chapter 2 and permits to simulate the partition function of the random-cluster model

$$Z = \sum_{A \subseteq G} q^{k(A)} \prod_{e \in A} v_e. \quad (6.8)$$

for a planar lattice.

We let A be the moves that use the ASM dynamics, i.e. to add a particle random on the sites of the sandpile and relax the configuration, and S the move that uses the Sweeny dynamics, i.e. to add or delete a bond with the dynamics presented in 5.3. Then we collect the dynamics together as presented in section 6.3 with $A=ASM$ and $B=S$, in particular we choose to boost the Sweeny dynamics that is slow in our region of investigation. We choose the threshold value for each simulation in order to obtain a balance between the boosted Sweeny move and the

ASM moves. The whole code is written in C-language, without the help of special libraries.

The crucial point of the algorithm consists in the possibility to pass, whenever necessary, back and forth between the representation in terms of height variables of the sandpile and the representation in terms of bond variables of the random-cluster model. This result is obtained constructing a function to map each connected cluster of bonds of the configuration in the ASM height's structure associated by the inverse of the burning test presented in section 2.4.2. In order to obtain a sort of invariance under rotation, or at least to decrease the influence of the prescription rule (e.g. NESW) in the function that perform the bijection between sandpile and bond configurations, we choose to update randomly distinctly for each site these regulations every time we need to use this function. Furthermore we note that the sandpile model and the spanning tree obtained via burning test, are not settled in the graph where is defined the random-cluster model, but in its dual. Thus we parallelly update the direct and planar-dual graphs during the simulation, in order to use one or the other according to the type of move we are doing. During the description of the burning test, it came out the particular task of the site burnt at time 0, in the burning test language, this site is called the *sink* of the graph. This site can be represented as a set of sites connected with each other, each one connected with at least one site on the boundary of the ASM cluster, and they are the initial points to construct all the burned zone, in the burning process. These sites are divided from the unburnt sites at time 0 by the bonds of the dual spanning tree associated to the spanning tree obtained with the burning test, that in our framework are the bonds of the random-cluster model. This shows how a cluster is completely surrounded by a burned profile. Thus we have that the basic action of the Sweeny dynamics, to add or delete an edge, corresponds in an ASM point of view, to modify the burned profile, in particular deleting a bond as the result to create a burned profile departing from the sites endpoints of the corresponding direct edge on the sandpile and adding a bond corresponds to remove the internal burned profile that the bond disconnects. A challenge of the algorithm is to update this part of the structure with a low-complexity procedure.

6.5 Numerical results

After writing and testing the computer program, we performed simulations of the model on an $L \times L$ square lattice for different sizes L and different temperatures T . The fact that the model is settled in an open square lattice, with no periodic conditions, does not allow to study many variables and correlation function for which the lack of symmetry makes very difficult the evaluation.

We define on the lattice the following local observables, for a configuration with set of bonds E and with heights of the sandpile $\{z_i\}$:

a- the local *bond occupation* n_e

$$n_e = \begin{cases} 1 & \text{if } e \in A \\ 0 & \text{otherwise} \end{cases} \quad (6.9)$$

b- the local *bond burnt* property b_e

$$b_e = \begin{cases} 1 & \text{if } e \text{ is burnt} \\ 0 & \text{otherwise} \end{cases} \quad (6.10)$$

we say an edge $e \in E$ is burnt if the corresponding dual edge $e' = ij \in E^*$ is such that its endpoints i and j are burnt.

c- the local *burnt site* property b_i

$$b_i = \begin{cases} 1 & \text{if } i \text{ is a burnt site} \\ 0 & \text{otherwise} \end{cases} \quad (6.11)$$

Using these local variables, and the further variable z_i that is defined, as usual, as the height in each site i (say, $z_i = 5$ if $b_i = 1$), we define the following functions:

$$B_e(t, \Delta t) = \sum_{e \in E} |b_e^{(t)} - b_e^{(t+\Delta t)}| \quad (6.12a)$$

$$N_e(t, \Delta t) = \sum_{e \in E} |n_e^{(t)} - n_e^{(t+\Delta t)}| \quad (6.12b)$$

$$Z_i(t, \Delta t) = \sum_{i \in V} \delta(z_i^{(t)}, z_i^{(t+\Delta t)}) \quad (6.12c)$$

$$B_i(t, \Delta t) = \sum_{i \in V} \delta(b_i^{(t)}, b_i^{(t+\Delta t)}) \delta(b_i^{(t)}, 1) \quad (6.12d)$$

These functions are a particular combination of the autocorrelation functions, for the observables defined in (a,b,c,d), translated and rescaled. The fact that in they can be expressed as sum and not products comes from the particular possible values of the local observables (0,1). Furthermore, they have different limits for $\Delta t \rightarrow \infty$ and $\Delta t \rightarrow 0$. We summarize the different limits in this tabular

	$\Delta t \rightarrow 0$	$\Delta t \rightarrow \infty$
B_e	0	$2y(1-y)L^2$
N_e	0	$L^2/2$
Z_i	L^2	$a + \varkappa^2$
B_i	$\varkappa L^2$	$\varkappa^2 L^2$

where

$$y = \text{prob}(b_e = 1) = \langle b_e \rangle \quad (6.13a)$$

$$\varkappa = \text{prob}(b_i = 1) = \langle b_i \rangle \quad (6.13b)$$

$$a = (1 - \varkappa)^2 \sum_{z=0}^3 p^2(z) \quad (6.13c)$$

where the $p(z)$ are the probabilities to have height z in the steady state computed by Priezhev [25] and take values

$p(0)$	0.074
$p(1)$	0.174
$p(2)$	0.307
$p(3)$	0.446

We collected the data to study these functions in various run at sizes

$$L = 64, 88, 128 \quad (6.14)$$

and temperature values

$$T = 0.04, 0.05, 0.06, 0.07, 0.08, 0.09 \quad (6.15)$$

To study the real improvement from a purely Sweeny dynamics, we collected the data for both the simulations with the ASM dynamics and the complete algorithm just presented. The data were taken every fixed interval of steps $(\Delta t)_{min}$ and postprocessed after the end of the runs. We present the plot of the data in figure 6.2, where in the x -axis is reported the different Δt values and the values of the functions are plotted, for all the t available, further is also drawn the curve that fit the data obtained as explained in the following.

To compute the curve for the fit of the data we first fit them with a single exponential with parameters a_1, b_1 and c_1

$$a_1 + b_1 e^{-\frac{x}{c_1}} \quad (6.16)$$

The data for the dynamics with both ASM and Sweeny moves fit well the single exponential, but the ones obtained with only the Sweeny dynamics clearly show a multiplicity of characteristic times C_α . Indeed looking at the data plots for the Sweeny dynamics is clearly visible an elbow in the curve, this represent the fact that the trend of the curve could not be obtained with a single exponential but at least with a superposition of two of them, one that give the trend for $\Delta t \rightarrow 0$ the other for $\Delta t \rightarrow \infty$. But to have a comparable result we have to do the fit with two exponentials also for the data of the composed dynamics, although they were well fitted by a single exponential. At this point we fit the data with a combination of two exponentials, with 5 parameters, a_1, b_1, c_1, b_2 and c_2

$$a_1 + b_1 e^{-\frac{x}{c_1}} + b_2 e^{-\frac{x}{c_2}} \quad (6.17)$$

Using this procedure we succeed in the task of fitting the data in a convincing way, but the errors in the parameters does not permit to use them as indicators of the real improvement obtained with our algorithm (in other words, the 5 parameters have huge cofluctuations, the non-diagonal elements of the correlation matrix for the fit parameters being not far from ± 1). Although the data plots clearly present

a decreasing autocorrelation time for the Sweeny dynamics to its union with the ASM dynamics, we have to find a better indicator instead of the fit parameters. Thus we decided to study quantities that better represent the curve, as the area below the curve, that can be obtained by combination of the fit parameters. In particular we have that the area can be obtained by the relation

$$b_1 c_1 + b_2 c_2 = \text{Area} \quad (6.18)$$

Another possible quantity indicator of the shape of the curve is the typical extension in the horizontal axes, i.e. $\langle \Delta t \rangle$ where times the area that is obtained as

$$b_1 c_1^2 + b_2 c_2^2 = \langle \Delta t \rangle \text{Area} \quad (6.19)$$

The value of $\langle \Delta t \rangle$ indicate how fast the curve is decreasing and thus it is a good indicator for the autocorrelation time. So we studied the combination

$$\langle \Delta t \rangle = \frac{b_1 c_1^2 + b_2 c_2^2}{b_1 c_1 + b_2 c_2} \quad (6.20)$$

Each value of $\langle \Delta t \rangle$ corresponds to a different observable in a given simulation. We report in figure 6.3 the results found with the simulations done for these variables, in the x -axis are reported the different temperatures of the various simulations and the height of the points corresponds to their value. We note a scaling of order 2 for almost every variable from the data set with Sweeny to the one with also ASM dynamics. In particular the observable n_e presents a clear improvement due to the ASM dynamics. Indeed, as displayed in figure 6.2 in the third pair of plots, the autocorrelation time evidently decreases when the ASM dynamics is introduced. The same result can be deduced looking at figure 6.3, there $\langle \Delta t \rangle_{n_e}$ is represented by light blue dots, and is evident that it is bigger than the value of $\langle \Delta t \rangle$ for the others observables. However, in the plots for the collected dynamics, all the observables have similar value for $\langle \Delta t \rangle$, this shows how n_e has definitely unfreezed.

We display also a figure of the typical configuration for a 128×128 lattice at temperature 0,07 in figure 6.4. In figure are traced the lines corresponding to the bonds of the random-cluster model and each elementary square is filled with a colour representing its height or its burning state, the scale of colours is

$z_i = 0$  $z_i = 1$  $z_i = 2$  $z_i = 3$  z_i burnt 

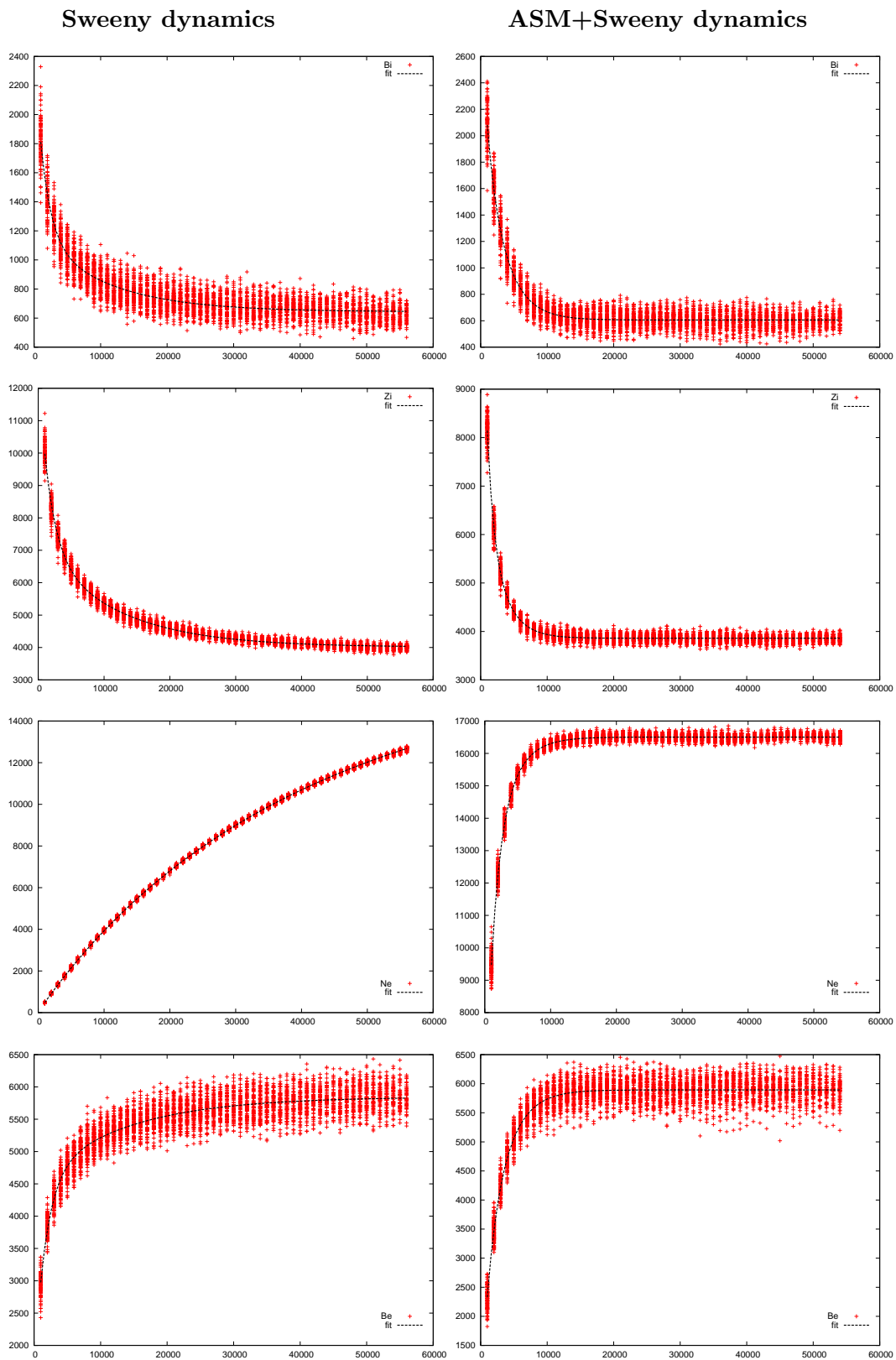
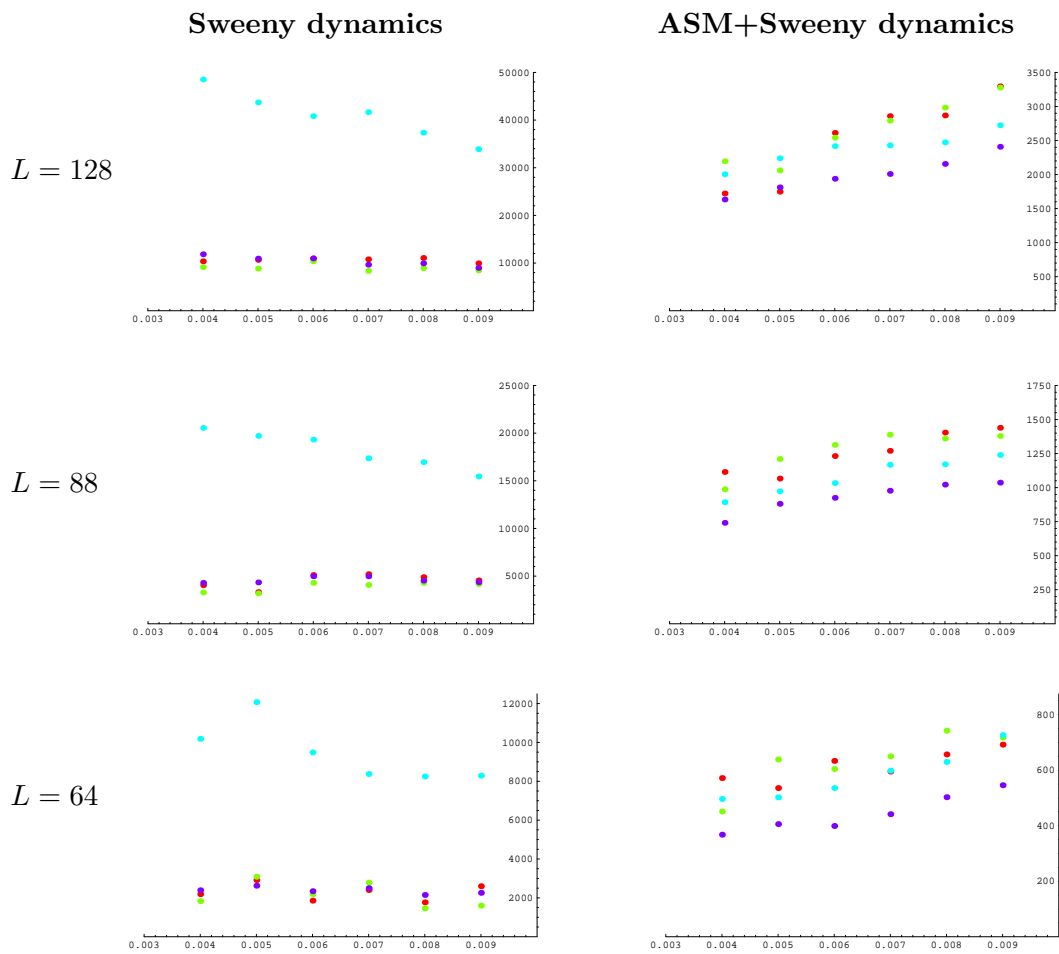


Figure 6.2 Plot of the data corresponding to a simulation for a lattice with parameters $L = 128$ at $T = 0.07$

Figure 6.3 Plot of the results for the $\langle \Delta t \rangle$

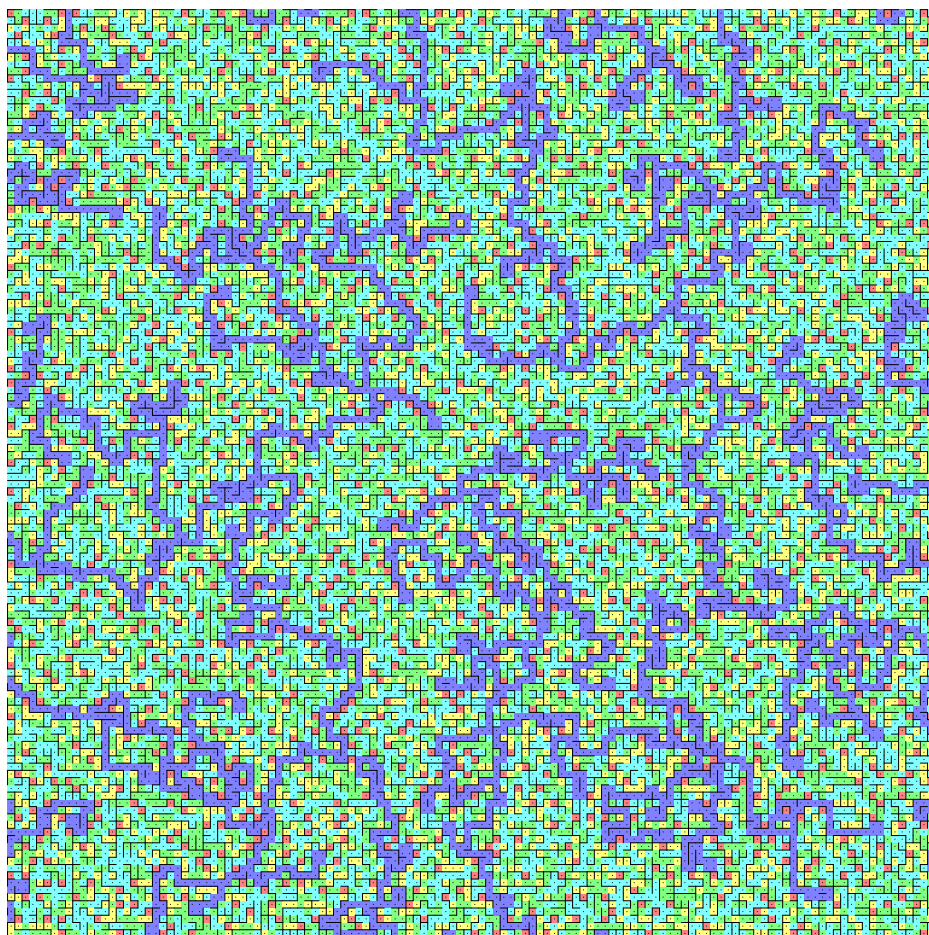


Figure 6.4 Typical configuration of heights and bonds for a lattice of size $L = 128$ at $T = 0.07$

Ringraziamenti

Eccomi alla fine, dopo queste ultime settimane di lavoro forzato sto per mettere un punto a chiusura delle mie fatiche. Credo però che non sarei qui ora se non grazie all'aiuto di alcune, anzi di molte persone. . .

Prima di tutto devo ringraziare Andrea, il mio correlatore, che mi ha seguito in questi mesi. Non credo di essere stato perfetto, mai, ma credo invece che quel poco di buono che sono riuscito a fare non sarebbe stato possibile senza il suo aiuto. La sua passione nel fare le cose, il suo entusiasmo nell'affrontare nuovi argomenti, sono stati un ingrediente essenziale perchè non mi lasciassi prendere dallo sconforto quando questo stava per assalirmi.

Subito di seguito voglio ringraziare il prof. Caracciolo, del quale ammetto ho avuto, per lungo tempo, soggezione e timore, ma che, con poche parole è sempre riuscito a chiarire i miei dubbi, a stimolare la mia attenzione e a farmi affrontare i problemi dalla giusta angolazione.

Un grazie speciale va ora alla mia famiglia: a mia mamma, mio papà e mia sorella. Loro come nessun'altro mi sono stati vicini in *ogni* momento, mi hanno *sempre* sostenuto quando ne ho avuto bisogno e hanno *sempre* creduto in me anche quando io stesso avevo perso la più basilare stima di me stesso, grazie di cuore!

Non posso ora mancare di ringraziare quel gruppo di pazzi fisici, e non, che mi hanno sopportato in questi anni di univertità e ancor di più in questi ultimi mesi: LucaRoma il mio lussemburghese preferito che mi ha ascoltato, e che ho ascoltato, nei momenti più disparati, Luca "el Tripon" col quale riesco sempre a scontrarmi ma per fortuna anche a riconciliarmi, Jo il cernuschese noto per la sua forza erculeica, Ricky che cerca sempre di tirarmi su e strapparmi un sorriso, Marco che con il suo innato cinismo mi ha fatto capire che i peli sulla lingua a volte possono essere superflui, GioViola compagno di studi che mi ha aiutato negli esami più difficili, il Sanghi che con la sua filosofia ci ha permesso di sopravvivere a un'interrail che sembrava una gita del manicomio, la Dani che si è rivelata è vera amica, con la parola giusta nei momenti giusti, Boris, la nostra greca ufficiale, Alice e Claudia, le mie due tesiste preferite, che forse a volte si devono sorbire i miei scleri, ma che fortunatamente mi sopportano e mi capiscono, navigando nella mia stessa barca, Ale Mesisca che mi ha seguito fin dagli inizi, il mio milanese d.o.c. preferito, Alex che mi ricorda che la potenza di un 2000 turbo non e' da sottovalutare, Alebughi che si è sorbita i miei monologhi senza mai tirarsi indietro, Olivia ed Elisa, le nostre donne ufficiali di fisica, che nel bene e nel male sono sempre con noi tra queste

quattro mura. A questo punto proseguo con una lista, forse non esaustiva ma con l'aspirazione di esserlo almeno in parte, grazie: Paolo (rasta), Philip, quelli di teolaur, il Chiari, la Ela (e tutta la vecchia guardia, Alice, Zamu e gli altri), Claudia (detta anche put_puri), Blazar, Jacopo, Davideg, il Cesco, Sandro, Karrots, la Fede, la Yle, la Kia, Maks, Marina, laFumi, Paul, Sofia (la mia ultima coinquilina), Nico, DavideF, Andrea (beb0s), Barbara, il Leone, Leo, Fradp, Teobina e Agenore.

Anche se spesso la mia permanenza varallese si limita a poche ore nel finesettimana, tornare a casa è sempre un piacere grazie ai miei amici. . . So che ovunque vada, quando torno loro mi aspettano. Grazie. So che un elenco è riduttivo ma è anche meglio che niente no? Gio, ti conosco da quando siamo entrambi alti la metà di quanto siamo ora ne abbiamo passate tante assieme, e ne passeremo ancora!, Paolo, Paulì, guarda che voglio venire presto alla tua di laurea!, Gigi, sono o non sono una gran comparsa!, Ari che mi ha sopportato questi ultimi due anni. . . e chi mi conosce sa quanto possa essere stato difficile, Andre, il mio coinquilino storico, vedi di tenermi un posto nel mondo del lavoro, la Ceci, la mia designer preferita, Alby il mio grande aiuto-CR, Agne, Chicco, Carlo, RastaMax, Puccia, Go, Ferra, Efrem, Gianni, Giorgio, Ivan, Laura, Vero, Marta, Cacaito, Zaira, Max, Fra, Jula, Elena, Sabrina, Marta, Louis, Carla, Boro e Vere.

Un grazie va anche ai miei parenti: nonne, zii e cugini. Un abbraccio forte alla nonna Teresa e alla nonna Carla, all'Antonio, la Sandra e i miei cuginetti Vitty e Eugi, e poi all'Angi, l'Augusto, la Rosalba, il Nico, la Fede, la Marta, la Francis e i miei due cugini aquisiti Davide e Mauro. Ma anche grazie ai miei parenti torinesi, anche se non ci vediamo spesso vi tengo sempre nel cuore.

Non posso dimenticare il mio gruppo scout e tutto quello che mi ha dato fin da quando sono piccolo. . . E quindi grazie a tutti loro, grazie Piui e Maria (che mi avete sopportato come CR e aiuto), Caba e Max (i momenti passati insieme alle route saranno sempre indimenticabili), Eugi, Don GianPaolo, Federica, Umberto, Piero e tutta la coca, anche se a volte sono stato una gatta da pelare mi avete dato tanto, e tutti quelli coi quali ho vissuto i miei anni di reparto e clan; per ultimi ringrazio tutti i miei ragazzi, il mio reparto, solo al pensiero di lasciarlo l'anno prossimo mi viene il magone, spero di aver lasciato qualcosa di buono a tutti loro anche se mai quanto quello che loro sono riusciti a dare a me, grazie!

Grazie anche al professor Urban e alla professoressa Caratti, anche a loro devo molto, senza di loro, senza i loro preziosi insegnamenti, non sarei arrivato dove sono arrivato oggi, non vi dimenticherò.

Ora è il momento finale, grazie al bar di fisica, Natty, Angelo, Gaetano, il vostro caffè ha saputo tenermi sveglio anche nei momenti più difficili, grazie a tutti i pazzi di fisica e dintorni, la preparata, moreno, la pazza di metodi e la pazza delle macchinette, grazie a quei simpaticoni che hanno scritto il mio nome su una colonna dell'aula occhialini, seguito da parole non molto simpatiche, grazie alla Tremenda, la Bea, il Teo, il bianchino-nerino, l'Achille e la Milla, grazie alla bella musica di Guccini, gli Afterhours e i Pearl Jam, grazie ai miei anticorpi che mi hanno salvato in molte occasioni, grazie alle mie innumerevoli biciclette, ormai tutte rubate o passate a miglior vita, grazie al microbirrifico di Lambrate, all'eastend

e allo Union, che mi hanno permesso di svagarmi quando ce n'era bisogno, grazie anche a Milano, alle sue strade, le sue serate che mi mancheranno sempre, infine ringrazio tutti quelli che ho dimenticato ma che sanno di meritare di essere citati in queste pagine, grazie.

E ora ringrazio Lei, perchè ha reso questi ultimi due anni speciali, *super*...

... grazie Luci.

Bibliography

- [1] S. Caracciolo, J.L. Jacobsen, H. Saleur, A.D. Sokal and A. Sportiello, *Fermionic field theory for trees and forests*, Phys. Rev. Lett. **93** (2004) 080601, [cond-mat/0403271](#)
- [2] G. Parisi and N. Sourlas, *Random magnetic fields, supersymmetry, and negative dimensions*, Phys. Rev. Lett. **43** 744-5 (1979)
- [3] J.G. Propp and D.B. Wilson, *Exact sampling with coupled Markov chains and applications to statistical mechanics*, Rand. Struct. Alg. **9** 223-252 (1996)
- [4] D. Dhar and S.N. Majumdar, *Equivalence between the Abelian sandpile model and the $q \rightarrow 0$ limit of the Potts model*, Physica A **185** 129-145 (1992)
- [5] Y. Deng, T.M. Garoni and A.D. Sokal, *Ferromagnetic phase transition for the spanning-forest model ($q \rightarrow 0$ limit of the Potts model) in three or more dimensions*, Phys. Rev. Lett. **98** (2007) 030602, [cond-mat/0610193](#); *Critical speeding-up in a local dynamics for the random-cluster model*, [cond-mat/0701113](#).
- [6] R. Bak, C. Tang and K. Wiesenfeld, *Self-organized criticality: An explanation of the $1/f$ noise*, Phys. Rev. Lett. **59** 381-4 (1987)
- [7] D. Dhar, *Self-organized critical state of sandpile automaton models*, Phys. Rev. Lett. **64** 1613-6 (1990)
- [8] D. Dhar, *Theoretical studies of self-organized criticality*, Physica A **369** 29-70 (2006)
- [9] D. Dhar and S.S. Manna, *Inverse avalanches in the Abelian sandpile model*, Phys. Rev. E **49**, 2684-87 (1994)
- [10] M. Sweeny, *Monte Carlo study of weighted percolation clusters relevant to the Potts model*, Phys. Rev. B **27** 4445-55 (1983)
- [11] D. Dhar, P. Ruelle, S. Sen and D.-N. Verma, *Algebraic aspects of Abelian sandpile models* J. Phys. A: Math. Gen. **28** 805-831 (1995) [cond-mat/9408022v1](#).
- [12] R.H Swendsen and J.-S. Wang *Nonuniversal critical dynamics in Monte Carlo simulations*, Phys. Rev. Lett. **58** 86-88 (1987)

- [13] G. Kirchhoff, *Über die Auflösung der Gleichungen, auf welche man bei der Untersuchung der linearen Verteilung galvanischer Ströme geführt wird*, Ann. Phys. Chem. **72** 497 (1847)
- [14] C. Godsil and G. Royle, *Algebraic Graph Theory*, Springer-Verlag (2001)
- [15] R. Diestel, *Graph Theory*, Springer-Verlag (2005)
<http://www.math.uni-hamburg.de/home/diestel/books/graph.theory/>
- [16] N. Biggs, *Algebraic Graph Theory*, Cambridge University Press (1974)
- [17] C.M. Fortuin and P.W. Kasteleyn, *On the random-cluster model. I. Introduction and relation to other models*, Physica **57** 536-564 (1972)
- [18] M. Creutz, *Abelian Sandpiles*, Comp. in Physics **5** 198-203(1991); *Abelian Sandpiles*, Nucl. Phys. B (Proc. Suppl.) **20** 758-761 (1991)
- [19] M. Creutz, *Xtoys: cellular automata on xwindows*, Nucl. Phys. B (Proc. Suppl.) **47** 846-849 (1996)
cond-mat/9408022v1
<http://thy.phy.bnl.gov/www/xtoys/xtoys.html>
- [20] B. Nienhuis, *Exact Critical Point and Critical Exponents of $O(n)$ Models in Two Dimensions*, Phys. Rev. Lett. **49**, 1062-1065 (1982)
- [21] J. Zinn-Justin, *Quantum Field Theory and Critical Phenomena*, 3rd ed. (Clarendon Press, Oxford, 1996)
- [22] N. Jacobson, *Basic Algebra*, (W.H. Freeman and Company, San Francisco, 1974)
- [23] H.N.V. Temperley in *Combinatorics, Proceedings of the British Combinatorial Conference*, London Mathematical Society Lecture Notes, Series vol. **13**, 202-204 (1974)
- [24] L. Chayes and J. Machta, *Graphical representations and cluster algorithms II*, Physica A **254**, 477 (1998)
- [25] V.B. Priezzhev, *Structure of Two-dimensional Sandpile. I, Height Probabilities*, J. Stat. Phys. **74**, 955 (1994)